The medical threat of mamba envenoming in sub-Saharan Africa revealed by genus-wide analysis of venom composition, toxicity and antivenomics profiling of available antivenoms

Ainsworth, Stuart; Petras, Daniel; Engmark, Mikael; Süssmuth, Roderich; Rowley, Paul; Wuster, Wolfgang; Dorrestein, Pieter C.; Arias, Ana Silvia; Gutiérrez, José Maria; Harrison, Robert A.; Casewell, Nicholas R.; Calvete, Juan J.

Journal of Proteomics

DOI:
10.1016/j.jprot.2017.08.016

Published: 10/02/2018

Peer reviewed version

The medical threat of mamba envenoming in sub-Saharan Africa revealed by genus-wide analysis of venom composition, toxicity and antivenomics profiling of available antivenoms

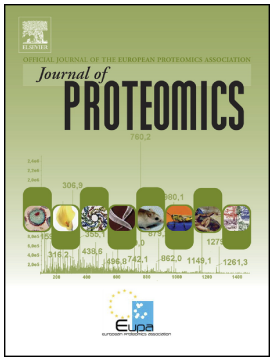

Stuart Ainsworth, Daniel Petras, Mikael Engmark, Roderich D. Süssmuth, Gareth Whiteley, Laura-Oana Albulescu, Taline D. Kazandjian, Simon C. Wagstaff, Paul Rowley, Wolfgang Wüster, Pieter C. Dorrestein, Ana Silvia Arias, José M. Gutiérrez, Robert A. Harrison, Nicholas R. Casewell, Juan J. Calvete

PII: S1874-3919(17)30303-2
DOI: doi: 10.1016/j.jprot.2017.08.016
Reference: JPROT 2927

To appear in: *Journal of Proteomics*

Received date: 5 July 2017
Revised date: 5 August 2017
Accepted date: 22 August 2017

Please cite this article as: Stuart Ainsworth, Daniel Petras, Mikael Engmark, Roderich D. Süssmuth, Gareth Whiteley, Laura-Oana Albulescu, Taline D. Kazandjian, Simon C. Wagstaff, Paul Rowley, Wolfgang Wüster, Pieter C. Dorrestein, Ana Silvia Arias, José M. Gutiérrez, Robert A. Harrison, Nicholas R. Casewell, Juan J. Calvete , The medical threat of mamba envenoming in sub-Saharan Africa revealed by genus-wide analysis of venom composition, toxicity and antivenomics profiling of available antivenoms, *Journal of Proteomics* (2017), doi: 10.1016/j.jprot.2017.08.016

The medical threat of mamba envenoming in sub-Saharan Africa revealed by genus-wide analysis of venom composition, toxicity and antivenomics profiling of available antivenoms

Stuart AINSWORTH[1,*], Daniel PETRAS[2,3,*], Mikael ENGMARK[4], Roderich D. SÜSSMUTH[3], Gareth WHITELEY[1], Laura-Oana ALBULESCU[1], Taline D. KAZANDJIAN[1], Simon C. WAGSTAFF[5], Paul ROWLEY[1], Wolfgang WÜSTER[6], Pieter C. DORRESTEIN[2], Ana Silvia ARIAS[7], José M. GUTIÉRREZ[7], Robert A. HARRISON[1] Nicholas R. CASEWELL[1,$], Juan J. CALVETE[8,$]

[1] Alistair Reid Venom Research Unit, Parasitology Department, Liverpool, School of Tropical Medicine, Pembroke Place, Liverpool L3 5QA, United Kingdom

[2] University of California San Diego, Skaggs School of Pharmacy & Pharmaceutical Sciences, 9500 Gilman Dr, La Jolla, CA 92093, USA

[3] Technische Universität Berlin, Institut für Chemie, Straße des 17.Juni 124, 10623 Berlin, Germany

[4] Technical University of Denmark, Department of Bio and Health Informatics, 2800 Kgs. Lyngby, Denmark

[5] Bioinformatics Unit, Parasitology Department, Liverpool School of Tropical Medicine, Pembroke Place, Liverpool L3 5QA, United Kingdom

[6] Molecular Ecology and Fisheries Genetics Laboratory, School of Biological Sciences, Bangor University, Bangor LL57 2UW, United Kingdom

[7] Instituto Clodomiro Picado, Facultad de Microbiología, Universidad de Costa Rica, San José, Costa Rica

[8] Instituto de Biomedicina de Valencia, Consejo Superior de Investigaciones Científicas (CSIC), Jaume Roig 11, 46010 Valencia, Spain

Running title: Genus-wide analysis of mamba venoms

Keywords: Genus *Dendroaspis*; mamba phylogeny reconstruction; top-down snake venomics; venom gland transcriptome; venom toxicity; genus-wide antivenomics; sub-Saharan antivenoms.

*These authors contributed equally to this work

[$] Corresponding authors. For questions on venom gland transcriptomics, contact Nicholas R. Casewell (Nicholas.Casewell@lstmed.ac.uk); For issues related to snake venomics and antivenomics, contact Juan J. Calvete (jcalvete@ibv.csic.es).

SUMMARY

Mambas (genus *Dendroaspis*) are among the most feared of the medically important elapid snakes found in sub-Saharan Africa, but many facets of their biology, including the diversity of venom composition, remain relatively understudied. Here, we present a reconstruction of mamba phylogeny, alongside genus-wide venom gland transcriptomic and high-resolution top-down venomic analyses. Whereas the green mambas, *D. viridis*, *D. angusticeps*, *D. j. jamesoni* and *D. j. kaimosae*, express 3FTx-predominant venoms, black mamba (*D. polylepis*) venom is dominated by dendrotoxins I and K. The divergent terrestrial ecology of *D. polylepis* compared to the arboreal niche occupied by all other mambas makes it plausible that this major difference in venom composition is due to dietary variation. The pattern of intrageneric venom variability across *Dendroaspis* represented a valuable opportunity to investigate, in a genus-wide context, the variant toxicity of the venom, and the degree of paraspecific cross-reactivity between antivenoms and mamba venoms. To this end, the immunological profiles of the five mamba venoms were assessed against a panel of commercial antivenoms generated for the sub-Saharan Africa market. This study provides a genus-wide overview of which available antivenoms may be more efficacious in neutralising human envenomings caused by mambas, irrespective of the species responsible. The information gathered in this study lays the foundations for rationalising the notably different potency and pharmacological profiles of *Dendroaspis* venoms at locus resolution. This understanding will allow selection and design of toxin immunogens with a view to generating a safer and more efficacious pan-specific antivenom against any mamba envenomation.

INTRODUCTION

Snakebite is medical emergency requiring prompt treatment. This is very problematic in most areas of sub-Saharan Africa because it is the rural, remote farming communities that suffer most [1]. Snakebite victims are often several hours from the nearest health centre, which is frequently inadequately equipped to effectively manage these medical emergencies [2]. In these circumstances, the unusually rapid onset of potentially lethal respiratory paralysis in victims of mamba (family Elapidae, genus *Dendroaspis*) bites poses particularly severe challenges to attending physicians. Mambas are therefore among the most feared venomous snakes in sub-Saharan Africa [3, 4].

There are four species in the genus *Dendroaspis* (Greek for "tree snake"): *D. polylepis* (black mamba), *D. angusticeps* (eastern green mamba) *D. viridis* (western green mamba) and *D. jamesoni*, which consists of two subspecies, *D. j. jamesoni* (Jameson's mamba) and *D. j. kaimosae* (eastern or black-tailed Jameson's mamba) [5]. These are large snakes (to ~1.9 m for green mambas and over 3 m for black mambas), their collective distribution covers much of sub-Saharan Africa (Fig. 1) and, except for *D. polylepis*, they are mostly arboreal, sedentary, ambush predators [6, 7] preying primarily on arboreal prey, mostly birds.

All mambas possess debilitating, neurotoxic venom which in human envenomations can rapidly lead to fasciculations, ptosis, cardiovascular collapse, respiratory paralysis and death (in extreme cases, this can occur in as little as 45 mins) [3, 8, 9]. Fatality rates are high unless mechanical ventilation and antivenom are administered quickly [4, 8, 10]. The black mamba poses the greatest medical threat because it injects large quantities (0.30-0.58 ml) of fast-acting, highly neurotoxic venom. Due to its size and speed it is a formidable threat when alarmed. *Dendroaspis polylepis* is often found in open savanna (although it can be encountered resting or foraging in trees) and is a fast-moving, wide-ranging terrestrial hunter.

Its savanna distribution and terrestrial habits bring it into contact with Africa's subsistence farming communities, threatening their lives and livelihoods. The medical importance of mambas is highlighted by the widespread inclusion of mamba venom in the manufacture of various polyspecific antivenoms marketed for use in sub-Saharan Africa.

The composition of *D. polylepis* and *D. angusticeps* venoms have previously been investigated using either bottom-up [11, 12] and/or top-down [13] venomics approaches. These proteomic studies revealed these venoms are comprised of >200 pharmacologically active components representing a small number of toxin families, the majority being neurotoxins belonging to the non-enzymatic, post-synaptically acting three-finger toxin family (3FTx) and the pre-synaptically acting Kunitz-type serine proteinase inhibitor-like (KUN) toxins, known as dendrotoxins. Within the 3FTx family, structural homology is generally conserved, however, individual mamba 3FTxs types have diverse biological functions, such as: blocking muscular nicotinic cholinergic receptors (long or short chain post-synaptic α-neurotoxins), blocking muscarinic receptors (cardiotoxins, also known as muscarinic toxins), inducing fasciculations by blocking acetylcholinesterase (fasciculins), specifically blocking L-type calcium channels and inhibiting smooth muscle contraction and cardiac function (calciseptine), and inhibition of acid sensing ion channels (mambalgins) [14-17]. The *Dendroaspis*-specific dendrotoxins mediate their neurotoxicity via stimulatory release of ACh at pre-synaptic neuro-muscular nerve junctions through binding and blockade of voltage dependent K^+ channels [18, 19]. Mamba venoms contain other KUN toxins, such as calcicludine [20], which target voltage-dependent Ca^{2+} channels, essential for the control of smooth and cardiac muscle contraction. Other less abundant toxin families, such as snake venom metalloproteinases (SVMP), natriuretic peptides (NP) [21], mamba intestinal toxins

(MIT) [22] and phospholipases A_2 (PLA_2) [23], were also detected by proteomic analyses of mamba venoms [11, 13].

The proteomic analysis of venoms, or "venomics", allows for the identification and quantification of individual proteinaceous toxins, with proteoform and isoform differentiating resolution [24, 25]. However, a major limitation in prior *Dendroaspis* venomic approaches (and that of many other venomic analyses) is the lack of comprehensive, publicly available, toxin sequences underpinning protein-identity assignments. Venom gland transcriptomics provide a comprehensive amino-acid sequence description of potential venom composition within a species [26]. The increasing accessibility of high-throughput sequencing technology has enabled routine combined transcriptomic-venomic approaches, that provide detailed characterisation of the protein composition of venoms [27].

Here we present, to our knowledge, the first genus-wide transcriptomic-proteomic analysis of venom composition in mambas, including overviews of the venom proteomes of *D. viridis*, *D. j. jamesoni* and *D. j. kaimosae,* and revisiting the *D. polylepis* and *D. angusticeps* proteomics performed by [13], with new venom-gland transcriptomic datasets, revealing novel toxins. We have used this data to resolve *Dendroaspis* species-relationships, interpret venom-variation in the context of the species history and examine the genus-wide neutralising potential of polyspecific antivenoms available in sub-Saharan Africa to mamba venoms.

MATERIALS AND METHODS

Venoms and antivenoms

Venoms of the green mamba (*D. angusticeps*, Tanzania), the black mamba (*D. polylepis*, Tanzania), the Jameson's mamba (*D. jamesoni jamesoni*, Cameroon), the eastern or black-

tailed Jameson's mamba (*D. j. kaimosae*, Uganda) and the West African green mamba (*D. viridis*, Togo) were pooled from wild-caught specimens maintained in the Herpetarium of the Liverpool School of Tropical Medicine. Crude venoms were lyophilised and stored at 4 °C until analysis.

The following nine commercial antivenoms for the African market (Table 1), were investigated in this study: (a) SAIMR (South African Institute for Medical Research) Polyvalent Snake Antivenom from South African Vaccine Producers (Pty) Ltd., Republic of South Africa (batch number BC02645, expiry date 07/2016); (b) FAV-Afrique from Sanofi-Pasteur, France (batch number K8453-1, expiry date 06/2016); (c) EchiTAb-Plus-ICP® from Instituto Clodomiro Picado, Costa Rica (batch number 5370114PALQ, expiry date 01/2017); (d) Inoserp Panafricain™ from Inosan Biopharma, S.A., Spain (batch number 2VT08001, expiry date 08/2015); (e) Snake Venom Antiserum (Central Africa) from VINS Bioproducts Ltd., India (batch 12AS13002, expiry date 04/2017); (f) Snake Venom Antiserum (African) from VINS Bioproducts (batch 13022, expiry date 01/2018); (g) Snake Venom Antiserum (Pan Africa) from Premium Serums and Vaccines Pvt. Ltd., India (batch 062003, expiry date 01/2018); (h) Antivipmyn® Africa from Instituto Bioclon S.A. (batch DFB-150903, expiry date 09/2020); and (i) EchiTAbG from Micropharm (batch EOG000950, expiry date 04/2016).

RNA isolation and purification

Venom glands were dissected from single specimens of the five mamba species described above, three days after venom extraction, and processed as previously described ([28-30] for detailed methodology). Briefly, immediately following euthanasia, venom glands were dissected and were immediately flash frozen in liquid nitrogen and stored cryogenically prior

to RNA extraction. Venom glands were homogenised under liquid nitrogen and total RNA extracted using a TRIzol Plus RNA purification kit (Invitrogen), DNAse treated with the PureLink DNase set (Invitrogen) and poly(A) selected using the Dynabeads mRNA DIRECT purification kit (Life Technologies).

RNA Sequencing, assembly and annotation

RNA-Seq was performed as previously described [30]. Briefly, The RNA-Seq library was prepared from 50 ng of enriched RNA material using ScriptSeq v2 RNA-Seq Library Preparation Kit (epicenter, Madison, WI, USA), following 12 cycles of amplification. The sequencing library was purified using AMPure XP beads (Agencourt, Brea, CA, USA), quantified using the Qubit dsDNA HS Assay Kit (Life Technologies) and the size distribution was assessed using a Bioanalyser (Agilent). Each library was then multiplexed and combined, and sequenced on 5/6ths of a single lane (1/6th of a lane for each transcriptome) of an Illumina MiSeq, housed at the Centre for Genomic Research, Liverpool, UK. The ensuing read data was quality processed, first by removing the presence of any adapter sequences using Cutadapt (https://code.google.com/p/cutadapt/) and then by trimming low quality bases using Sickle (https://github.com/najoshi/sickle). Reads were trimmed if bases at the 3' end matched the adapter sequence for 3 bp or more, and further trimmed with a minimum window quality score of 20. After trimming, reads shorter than 10 bp were removed.

Paired-end read data were assembled into contigs using the *de novo* transcriptome assembler VTBuilder [31] executed with the following parameters: min. transcript length 150 bp; min. read length 150 bp; min. isoform similarity 96%. Assembled contigs were annotated with the BLAST2GO Pro v3 [32] using the blastx-fast algorithm with a significance threshold of 1e-5, to provide BLAST annotations (max 20 hits) against NCBI's non redundant (NR)

protein database (41 volumes; Nov 2015) followed by mapping to gene ontology terms, and Interpro domain annotation using default parameters. Post-annotation, contigs were grouped into three categories: (i) toxins (contigs with homology to sequences previously identified as pathogenic toxins), (ii) non-toxins (e.g. contigs matching sequences such as housekeeping genes) and (iii) unassigned (contigs where no matches were assigned or BLAST E-values <1e-5).

Top-down venomics

For top-down mass spectrometric analysis, venoms were dissolved in 1% formic acid (FA) in ultrapure water to a final concentration of 10 mg/mL, and centrifuged at 20,000 g for 5 min. To reduce disulfide bonds, 10 µL of venom were mixed with 10 µL of 0.5 M tris(2-carboxyethyl)phosphine (TCEP) and 30 µL of 0.1 M citrate buffer, pH 3, and incubated for 30 min at 65 °C. Samples were centrifuged at 20,000 g for 5 min and 10 µL of reduced and non-reduced samples were submitted to reverse-phase (RP) HPLC-MS/MS analyses. RP-HPLC- MS/MS experiments were performed on an Agilent 1260 HPLC system (Agilent, Waldbronn, Germany) coupled to an Orbitrap LTQ XL mass spectrometer (Thermo, Bremen, Germany). RP-HPLC separation was performed on a Supelco Discovery Biowide C18 column (300 Å pore size, 2 x 150 mm column size, 3 µm particle size). A flow rate of 0.3 mL/min was used and the samples were eluted with a gradient of 0.1% FA in water (solution A) and 0.1% FA in acetonitrile (ACN) (solution B): 5% B for 1 min, followed by 5-40% B for 89 min, and 40-70% for 20 min. Finally, the column was washed out with 70% B for 10 min and re-equilibrated at 5% B for 10 min. ESI settings were set to 11 L/min sheath gas, 35 L/min auxiliary gas, spray voltage, 4.8 kV, capillary voltage, 63 V, tube lens voltage, 135 V, and capillary temperature, 330 °C.

MS/MS spectra were obtained in data dependent acquisition (DDA) mode. FTMS measurements were performed with 1 micro scan and 1000 ms maximal fill time. AGC targets were set to 10^6 for full scans and to 3 x 10^5 for MS/MS scans. The survey scan and both data dependent MS/MS scans were performed with a mass resolution (R) of 100,000 (at m/z 400). For MS/MS, the two most abundant ions of the survey scan with known charge were selected. Normalised collision-induced dissociation (CID) energy was set to 30% for the first, and 35% for the second, MS/MS event of each duty cycle. The default charge state was set to z = 6, and the activation time to 30 msec. The mass window for precursor ion selection was set to 3 m/z. A window of 3 m/z was set for dynamic exclusion of up to 50 precursor ions with a repeat of 1 within 10 sec for the next 20 sec. For data analysis, .raw data were converted to .mzXML files using MSconvert of the ProteoWizard package (version 3.065.85) and multiple charged spectra were deconvoluted using MS-Deconv (version 0.8.0.7370). The maximum charge was set to 30, maximum mass was set to 50,000 Da, signal to noise threshold was set to 2 and m/z tolerance was set to 0.02 amu. Protein spectra matching was performed using TopPIC (http://proteomics.informatics.iupui.edu/software/toppic/) (version 1.0.0) against a non-redundant database comprising all NCBI *Dendroaspis* spp. full-length protein entries (165 sequences, 11th March 2015) and the full-length *Dendroaspis* spp. protein sequences translated from the five species-specific venom gland transcriptomic analyses. TopPIC mass error tolerance was set to 10 ppm. A false discovery rate (FDR) cut-off was set to 0.01. Maximal allowed unexpected PTMs were set to one. For intact mass feature finding and manual validation of protein spectra matches, the MS data were deconvoluted using XTRACT of the Xcalibur Qual Browser version 2.2 (Thermo, Bremen, Germany). Intact mass feature finding of both mono-isotopic deconvoluted reduced and native LC-MS runs was performed with MZmine 2 (version 2.2). A 1.0E4 signal intensity threshold was used for

MS1 peak picking. The mass alignment for the creation of extracted ion chromatograms (EIC) was performed with a minimum peak width of 30 sec, and 3.0E4 peak height. Mass error tolerance was set to 10 ppm. For chromatographic deconvolution, the baseline cut-off algorithm with a 1.0E4 signal threshold was applied. Maximum peak width was set to 2 min. Alignment of reduced and native protein masses and incorporation of protein-spectra matches was performed manually. Relative ion intensities of native venom proteins were calculated using the area under the curve of extracted ion chromatograms (EIC).

Multivariable statistic

Principal component analysis (PCA), using the percentages of the major toxins (Table 2) as a variable, was applied to explain determinants of compositional variation among venoms. PCA was performed in the Programming Language R (version 3.3.0, R Foundation for Statistical Computing, 2016) with the extension Graphic Package rgl (version 0.93.996), available from https://www.R-Project.org. Comparisons of intact masses among *Dendroaspis* species were visualised in a Venn diagram using software InteractiVenn [33].

Mamba phylogeny

To reconstruct the phylogeny of the five *Dendroaspis* taxa used in this study, we extracted the gene sequences of two mitochondrial genes, cytochrome *b* (*cytb*) and NADH dehydrogenase subunit 4 (ND4), from the venom gland transcriptome data. Transcriptomic-derived sequences were aligned with existing directly sequenced *Dendroaspis* sequences to confirm the identity of the transcriptome specimens and the correct assembly of the sequences. For phylogenetic analyses, we concatenated the *cytb* and ND4 sequences. We partitioned the data by gene and by codon position, and identified the best model of sequence evolution under the

Akaike Information Criterion (AIC) using MrModeltest [34]. For phylogeny reconstruction, we used MrBayes 3.2.2 [35]. We used corresponding sequences from the mitochondrial genome of the king cobra (*Ophiophagus hannah*; GenBank accession number EU921899), a putatively closely related elapid snake [36, 37], to root the tree. We ran the analysis for 5 x 10^6 generations using four simultaneous independent runs initiated with different random starting trees and sampling every 500 generations. Plots of lnL against generation time were inspected to determine the burn-in period, and trees generated prior to the completion of burn-in were discarded. As an additional safety margin, we discarded the first 5 x 10^5 generations.

Venom lethality testing

The venom median lethal dose (LD_{50}) was determined using WHO approved protocols [38]. Groups of five male CD-1 mice (18-20g) received an intravenous (iv) tail injection of varying doses of venom in 100 µL of 0.12 M NaCl, 40 mM phosphate, pH 7.2 (PBS), namely 27-60 µg/mouse (*D. angusticeps*), 10-45 µg/mouse (*D. j. jamesoni*), 2-40 µg/mouse (*D. j. kaimosae*), 2-14 µg/mouse (*D. polylepis*), and 12-40 µg/mouse (*D. viridis*). Twenty-four hours later, the number of surviving mice in each group was recorded. The venom LD_{50} (the amount of venom that kills 50% of the injected mice) and 95% confidence limits of each snake species was calculated using probits. Venom LD_{50} assays were performed at the Instituto Clodomiro Picado (San Joé, Costa Rica) using protocols approved by the Institutional Committee for the Use of Laboratory Animals (CICUA) of the University of Costa Rica (project 82-08).

Antivenomics

A second-generation immunoaffinity-based antivenomics approach was applied to examine immunoreactivity of the nine antivenoms listed in Table 1 towards venom proteins of the five *Dendroaspis* taxa. For each antivenom an immunoaffinity chromatography column was prepared following the protocol described previously [39]. For preparing the immunoaffinity chromatography matrix, 300 µL of CNBr-activated Sepharose™ 4B (GE Healthcare, Chicago, USA) were packed in Pierce disposable microcentrifuge spin columns (Thermo Scientific, Bremen, GER) and washed with 10 matrix volumes of cold 500 µL 0.1 mM HCl at 5 °C and twice with 500 µL coupling buffer (0.2 M $NaHCO_3$, 0.5 M NaCl, adjusted to pH 8.3). Antivenoms were dialysed against MilliQ® water using SpectraPor Membrane MWCO 3500 (Spectrum Laboratories, California, USA) to remove salts and preservative that could otherwise interfere with coupling to the matrix. Antivenoms were then lyophilised and reconstituted in coupling buffer. Concentrations of antivenom stock solutions were determined spectrophotometrically at λ = 280 nm using a 1-cm path-length cuvette and extinction coefficients of 1.36 and 1.48 for a 1 mg/mL concentration of IgG and $F(ab)'_2$, respectively [40]. Antivenoms were dissolved in a half-matrix volume of coupling buffer and incubated with the matrix for 4 h at room temperature. Antivenom coupling yield, estimated measuring the absorbance at 280 before and after coupling of the antivenom, were 8.0 mg (SAIMR polyvalent), 9.5 mg (FAV-Afrique), 9.9 mg (EchiTAb-Plus-ICP®), 9.3 mg (Inoserp Panafricain™), 9.1 mg (VINS, Central Africa), 8.3 mg (VINS, African), 9.8 mg (Premium Serums, Panafrican), 9.4 mg (Antivipmyn® Africa), and 9.5 mg (Micropharm, EchiTAbG). After coupling, the remaining reactive groups were blocked with 300 µL of 0.1 M Tris-HCl, pH 8.5 at room temperature for 4 h, and columns were alternately washed with 3x 300 µL volumes of 0.1 M acetate containing 0.5 M NaCl, pH 4.0-5.0, and 3x 300 µL volumes of 0.1

M Tris-HCl, pH 8.5. This procedure was repeated 6 times. Columns were then equilibrated with 5 volumes of PBS (20 mM phosphate buffer, 135 mM NaCl, pH 7.4) and incubated on a wheel mixer for 2 h at 25 ºC with 50 µg of crude mamba venom in 250 µL of PBS. Assuming an average mamba toxin molecular mass of 9.7 kDa, the calculated venom to antivenom mass ratios were 1:15 (SAIMR polyvalent), 1:17 (FAV-Afrique), 1:13 (EchiTAb-Plus-ICP®), 1:16 (Inoserp Panafricain™), 1:16 (VINS Central Africa), 1:15 mg (VINS African), 1:17 (Premium Serums, Panafrica), 1:17 (Antivipmyn® Africa), and 1:12 (Micropharm EchiTAbG). As specificity controls, 300 µL of mock CNBr-activated Sepharose™ 4B matrix incubated with venom, and a 300 µL CNBr-activated Sepharose™ 4B matrix control column coupled with 7.9 mg preimmune equine IgG were run in parallel.

Non-retained fractions were collected over three rounds of washing using 250 µL PBS, and immunocaptured proteins were eluted with 3 x 300 µL of elution buffer (0.1 M glycine-HCl, pH 2.0) and neutralised with 150 µL 1M Tris-HCl, pH 9.0. Non-retained and immunocaptured venom fractions were lyophilised, reconstituted in 40 µL of 0.1% TFA in MilliQ® water, and fractionated by reverse-phase HPLC using a Supelco/Sigma Aldrich Discovery® BIO Wide Pore C_{18} (15 cm x 2.1 mm, 3 µm particle size, 300 Å pore size) column using an Agilent LC 1100 High Pressure Gradient System equipped with a DAD detector. The column was run with a flow rate of 0.4 mL/min and proteins eluted with a linear gradient of 0.1% TFA in MilliQ® water (solution A) and 0.1% TFA in acetonitrile (solution B): isocratic at 5% solution B for 1 min, followed by 5-25% solution B for 5 min, 25-45% solution B for 35 min, and 45-70% solution B for 5 min. Protein was detected at 215 nm with a reference wavelength of 400 nm. Chromatographic peaks were integrated manually and the relative amounts of venom bound in each antivenom affinity column (% R_i) were determined

as R_i /(NR_i + R_i), where R_i is the sum of the peak areas in the retained venom fraction i and NR_i is the sum of the peak areas in the non-retained fraction of the same experiment.

Enzymatic PLA_2 fluorescent assay

To assess PLA_2 activity across all five mamba venoms we used an EnzChek™ Phospholipase A2 Assay Kit (#E10217, Fisher Scientific), following the manufacturer's instructions. Briefly, 10 μg of each venom were assayed in triplicate, for each experimental repeat. As a comparator and positive control respectively, 0.15 μg samples of *Naja melanoleuca* (forest cobra) venom and 1 μg samples of *Crotalus atrox* (western diamondback rattlesnake) venom were also measured, plus a negative control containing no venom. Different venom doses were required due to a considerable difference in PLA_2 activity between these venoms, so that the measured values would fall in the linear range of the standard curve. The standard activity curve was generated using 5, 4, 3, 2, 1 and 0 U/mL of bee PLA_2 enzyme supplied in the kit. Fifty microlitre samples were mixed with 50 μL of substrate mix and the reaction incubated in the dark for 10 min. End-point fluorescence was then measured on a FLUOStar Omega Instrument (BMG Labtech GmbH, Ortenberg, Germany) at an excitation wavelength of 485 nm and an emission wavelength of 520 nm. The negative control mean was subtracted from raw values for each sample and PLA_2 activity was calculated as (U/mL)/μg of venom, relative to the standard curve. To normalise across independent experimental repeats, the PLA_2 activity in each sample was divided by the PLA_2 activity of the *C. atrox* sample.

RESULTS

Dendroaspis phylogeny

To reconstruct the phylogeny of the five *Dendroaspis* taxa used in this study we aligned 1035 bp of the cytochrome b gene and 1218 bp of the ND4 gene. Consistent with protein-coding mitochondrial DNA sequences, the translation of these sequences revealed no unexpected indels, frameshifts or stop codons. The phylogeny recovered from the Bayesian analysis of the data is shown in Figure 2. Our results show a strongly supported sister-group relationship between *D. jamesoni* and *D. viridis*, with a robustly supported clade consisting of *D. polylepis* and *D. angusticeps* as its sister taxon. The data show little differentiation between the two recognised subspecies of *D. jamesoni*; *D. j. jamesoni* and *D. j. kaimosae* (p-distance = 0.02).

Overview of *Dendroaspis* venom-gland transcriptomes

Sequencing of venom gland transcriptomes, generated in a similar manner to transcriptomes described previously [30, 31], yielded 6,031,390 (*D. polylepis*), 4,326,295 (*D. angusticeps*), 4,199,700 (*D. viridis*), 4,425,097 (*D. j. jamesoni*) and 4,716,831 (*D. j. kaimosae*) trimmed, paired-end reads. These reads were subsequently assembled into 5,985 (*D. polylepis*), 4,527 (*D. angusticeps*), 3,679 (*D. viridis*), 4,288 (*D. j. jamesoni*) and 2,825 (*D. j. kaimosae*) distinct contigs. Post-annotation, contigs were grouped into three categories: toxins, non-toxins and unassigned, as described in the Materials and Methods. Figure 2 and Supplementary Tables S1-S5 display the number of transcripts and their relative expression contributions of each category for each venom-gland transcriptome. In line with previous snake venom gland transcriptomes (e.g. [31, 41]), toxin transcripts account for 25-56% of the

entire transcriptome expression levels, despite only comprising 2-4% of the total number of contigs (Supplementary Table S6).

Post-curation, the *D. polylepis* venom gland transcriptome contained 48 full-length or partial toxin transcripts, the majority belonging to the 3FTx (24 transcripts), KUN (10) and SVMP (10) protein families (Table S1; Table S6). Surprisingly, no PLA_2, prokineticin or cysteine-rich secretory protein (CRISP) transcripts were detected, although transcripts from presumed prokineticin pseudogenes (subsequently removed from analysis due to the presence of stop codons) were observed. In terms of expression, toxin transcripts were dominated by KUN (49% of total toxin transcript expression) and 3FTx (45%) families. *D. polylepis* was the only mamba species not to have 3FTx as the most highly expressed toxin class (Fig. 2). Highly expressed *D. polylepis* toxin mRNAs include those encoding Dendrotoxin I [UniProtKB/Swiss-Prot (http://www.uniprot.org/) accession code P00979] homolog (T1947_T4455) and short-neurotoxin 1 [P01416] (T1284) (4.1%), which account for 6.9% of the expression of all venom gland genes (Table S6) and are responsible for 30% and 18% of the total toxin proteome expression, respectively.

The curated *D. angusticeps* transcriptome consists of 48 individual full length or fragment transcripts, the majority belonging to the 3FTx (22), SVMP (13) and KUN (6) toxin families, with expression dominated by 3FTx family transcripts (71%) followed by KUN (14.5%) and natriuretic peptide precursors (6%) (Fig. 2; Table S2; Table S6). A homolog of the 3FTx fasciculin 2 [P0C1Z0] (T3547) is the most highly expressed *D. angusticeps* toxin (5.8% of total venom gland mRNAs, Table S2), followed by the 3FTx L-type calcium channel blocker toxin C10S2C2 [P25684] [43] (T4516_T0621_T0929; 2.8%) and muscarinic toxin 2 (P18328) [42] (2.4%) (Table S2).

D. viridis contained the largest (90 individual toxin transcripts) and most diverse set of toxin transcripts post-curation (Fig. 2, Table S3; Table S6). As with *D. polylepis* and *D. angusticeps*, the majority of the transcripts belong to the 3FTx (46), SVMP (24) and KUN (13) families (Table S6). Toxin transcript expression was dominated by 3FTxs (78%), followed by KUN (15%). There were two highly expressed 3FTx, a S5C4 [P01406] homolog (T3493_T3274) [43] and a synergistic-like venom protein S2C4 homolog [P01407] [44] (T0454.2_T3272/T1637, Table S3), representing 6.2% and 3.7% of the total venom gland mRNAs (Table S6), respectively.

The *D. j. jamesoni* venom gland transcriptome comprised transcripts from six toxin families, including 3FTx (22 transcripts), SVMP (11), KUN (6), PLA_2 (1), NP (1) and prokineticin (1) (Fig. 2, Table S4; Table S6). Toxin-specific expression was dominated by 3FTx (80%), followed by KUN (15%). Transcripts T3431_T3432 encoding a syngergistic-like venom 3FTx protein S2C4 [P01407] homolog [44] accounted for 18% of the total venom gland mRNA expression, and toxin S5C4 [P01406] homolog [43] for 13.5% (T3920_T3924_T3915, Table S4).

Finally, the *D. j. kaimosae* venom gland transcriptome has the smallest number of toxin-specific transcripts, 31 in total – although we note that this transcriptome, once assembled, consisted of the lowest number of contigs. Of these toxin-encoding transcripts, the majority were annotated as 3FTx (13), followed by SVMP (7), KUN (5), NP (2) and prokineticins (2), and a single PLA_2 transcript (Table S5; Table S6). *D. j. kaimosae* venom-gland toxin expression was dominated by 3FTxs (66%), KUN (15%) and prokineticin (14%) transcripts (Table S6). A short neurotoxin 1 [3S11_DENJA; P01417] [45] homolog (T0532_T2409_15.659, Table S5) is by far the most dominantly expressed toxin, accounting for 15.7% of the total venom gland mRNA expression (Table S5) (43% of the total toxin

expression), followed by dendrotoxin B-like (2.7% of the total venom gland mRNA expression) and two prokineticin transcripts (2.6% and 2.4%).

Despite the high number of individual SVMP transcripts detected across the mamba venom gland transcriptomes (Table S6), their expression levels are relatively low (0.2% to 3.5% total toxin expression) and the majority do not represent intact toxin-encoding genes, but instead are non-overlapping contigs that are partial length. Thus, contig numbers for this toxin type (unlike those for 3FTx, KUN, prokineticin, etc) are not a true representation of the number of toxin encoding genes.

Overview of top-down venomics

Venom-gland transcriptomic datasets enabled a global overview of potential venom composition within a species. This database also facilitated characterising the toxin proteoform composition of mamba venoms through a top-down venomics approach [13]. Reversed-phase HPLC separation and on-line high-resolution top-down MS/MS encompasing fractions 1-37 from *D. j. jamesoni*, *D. j. kaimosae*, and *D. viridis* venoms (Fig. 3), yielded good quality fragmentation spectra (Fig. 4), which enabled the identification of 62 (*D. j. jamesoni*), 71 (*D. j. kaimosae*), and 55 (*D. viridis*) venom proteoforms belonging to the 3FTx, KUN, NP, and prokineticin (previously found in the venom proteomes of *D. angusticeps* and *D. polylepis*) [11-13] toxin families, and proteoforms belonging to the PLA_2 toxin family (Table 2; Supplementary Tables S7-S12). The overwhelming majority of mamba venom proteomes (83-87%, Table 2) were comprised of toxins in the 6-9.8 kDa range. Generally, the proteomes of *D. viridis* and the Jameson's mambas, *D. j. jamesoni* and *D. j. kaimosae*, were strikingly similar in content, differing mainly in the abundance of individual components (Table 2, Fig. 3). Similar to the previously reported *D. angusticeps* venom proteome [13], *D.*

j. jamesoni, *D. j. kaimosae* and *D. viridis* all have 3FTx-dominated venoms (65.5% to 76.7% of the total proteome) (Fig. 3) However, unlike *D. angusticeps*, in which the most abundant venom toxin is DaF8 [P01404] (Tables 2 and S8), toxin homologs of S5C4 [P01406] were the most highly abundant toxin in each of the *D. j. jamesoni* (45.5%), *D. j. kaimosae* (44.6%) and *D. viridis* (40.1%) venoms (Fig. 3). Additionally, the dominant KUN protein in the *D. j. jamesoni* (12.5%) and *D. j. kaimosae* (8.9%) venoms was dendrotoxin I-like toxin, while in the *D. viridis* venom this was a homolog of dendrotoxin, C13S2C3 (2.1%) (Table 2, Fig. 3, Tables S9-S12).

The re-analysis of the top-down MS data gathered for *D. angusticeps* and *D. polylepis* venom proteomes against the revised, venom-gland transcriptome assisted *Dendroaspis* toxin sequence dataset (Table S13), confirmed the KUN I and K dominated venom of *D. polylepis* and the 3FTx DaF8 dominated venom of *D. angusticeps* [13]. Additionally, the quality of the assignments of previously reported venom components [13] was enhanced through the new database (highlighted sequences in Tables S7 and S8), resulting in higher sequence coverage and lower p-values. Our data also confirmed the absence of neurotoxin-1 in *D. angusticeps* venom. Highly conserved isoforms of this short-chain 3FTx, which exhibited the lowest LD_{50} for mice (0.08 mg/kg) among black mamba venom toxins [11], are present in *D. viridis* [P01418] (Table S9), *D. j. jamesoni* [P01417] (Table S10), and *D. j. kaimosae* [P01417] (Table S11), where they account for 3.5%, 8.3% and 0.9% of the respective venom proteome. New toxins were also identified, particularly associated with low abundant mass signals. Notably, this revision of the *D. angusticeps* top-down MS data against the *D. angusticeps* transcriptomic database identified low-abundance isoforms of a hitherto unknown α-neurotoxin structurally similar to short neurotoxin ACR78511 from *Drysdalia coronoides*

[46] (Table S8, native mass 6759.9 Da). The toxicity of this toxin requires detailed pharmacological studies.

Additionally, the revised *Dendroaspis* full length toxin database allowed for the assignment of low molecular mass peptides (m/z < 4500) as natriuretic peptides, by mass matching against the full-length sequences of the species-specific natriuretic peptide precursors (sequences T0959_DJJ, T1153_DV, T0090_DV, T2598_DJK, T0860_Da, T4515_Da, T1102_Dp, T0758_Dp, and T0440_Dp listed in Table S13). On the other hand, each mamba species contains several venom protein ions that remain unassigned. These corresponded to low molecular mass peptides (potentially toxin degradation products) and less abundant high molecular mass ions (range 23-50 kDa), which hypothetically could correspond to CRISP and/or SVMP transcripts observed in the venom gland transcriptomes, which have previously been observed in the *D. polylepis* venom [11], and 13-14 kDa components only detected in the non-reduced mass measurements, for which no fragmentation spectra were recorded.

Synergistic-type venom proteins of the 3FTx family have odd numbers of cysteines and have been reported to form dimeric arrangements, such as dimeric toxins S2C4 [P01407], C9S3 [P17696], and S6C6 [P25682] [44, 47]. 3FTxs similar to these dimeric toxins were identified in reduced venoms of *D. j. jamesoni* (S6C6, S2C4), *D. j. kaimosae* (S6C6), *D. angusticeps* (C9S3, S6C6), *D. viridis* (S6C6, S2C4) and *D. polylepis* (S6C6) (Supplementary Tables S7-S11), suggesting that some of the non-assigned 13-14 kDa proteins may corresponded to dimeric 3FTxs. Supporting this assumption, mass ions 13977.5, 14038.5, 14004.5 and 14019.6 Da, recorded in RP-HPLC fractions 10-12 of *D. angusticeps* venom (Fig. 1 of [13]) (Table S8), precisely match the masses calculated for a heterodimer of synergistic-like toxin C9S3 and synergistic-like toxin T1269_Da [7003.3 Da + 6976,4 (-2) Da

= 13977.7 Da], homodimeric synergistic-like toxin T1318_Da [2 x 7019.3 (-2) Da = 14036.6 Da], a homodimer of C9S3 [2 x 7003.3 (-2) Da = 14004.6 Da], and a heterodimer of synergistic-like toxins C9S3 and T1318_Da [7003.3 Da + 7019.3 (-2) Da = 14020.6 Da]. Similarly, the two synergistic-type venom proteins identified in *D. j. jamesoni* venom (T3431_Djj and T1949_Djj, Table S2) may form a native heterodimer [7056.32 Da + 7078.45 (-2) Da = 14132.77 Da] found in RP-HPLC fraction 12c (Fig. 3A, Table S10). For *D. viridis*, a synergistic-like sequence was assigned to T3091_DV ([~P01407, S2C4] 7112.43 Da) which eluted in RP-HPLC fraction 26 (Fig. 3C), but no mass corresponding to a dimeric molecule was measured. In accordance with the venom gland transcriptome, no synergistic-like protein was found in the venom of the black mamba, *D. polylepis*. On the other hand, this venom contained two protein homologues (T2931_Da and T0104_Da, Table S5) of *D. j. kaimosae* long-chain 3FTx S6C6 [P25682], each containing 11 cysteine residues, although no putative homo- or heterodimeric arrangement of T2931_Da and T0104_Da was detected.

A non-assigned mass of 14112.38 Da, recorded in *D. j. jamesoni* fraction 12a and which accounted for 2.2% of the total venom proteome (Table S10), may correspond to T0814_Djj, the only PLA_2 sequence identified in the corresponding venom gland transcriptome (M_{ave} calculated for A20-G145 with all cysteine residues engaged in 7 disulphide bonds = 14111.94 Da). The same molecule was identified in *D. viridis* and *D. j. kaimosae* venoms, where its relative abundance was estimated at 0.16% and 1.8% of the respective venom proteomes (Tables 2, S9 and S11). Furthermore, contradicting previous assignments [13], our current omic data do not support the presence of PLA_2s in the venom proteomes of *D. polylepis* and *D. angusticeps.* It is unusal for venomous snakes to have little or no PLA_2 in their venom. However, we confirmed the paucity of PLA_2 in mamba venoms by fluorescent enzymatic PLA_2 assay. The results of this assay (Fig. 5) are in broad agreement

with our omic data, with each venom displaying neglible (*D. angusticeps*) or extremely low PLA_2 activity (*D. j. jamesoni, D. j. kaimosae, D. viridis* and *D. polylepis*) (Fig.5). To place these results into context, we compared them with the venom of another African elapid, the forest cobra (*Naja melanoleuca*), which we found exhibits at least 300-fold greater PLA_2 activity compared to the most active of the five mamba venoms (*D. polylepis*). To our surprise, sequence analysis of the PLA_2 detected in the venom gland transcriptome revealed homology to the colubrid-type group IIE PLA_2 [48], and not the typical group IB PLA_2 toxins found in other elapid snakes [49]. In combination, this data strongly suggests that mambas have lost their group I PLA_2 toxins and have little to no venom PLA_2 activity.

In previous work, the lack of comprehensive species-specific sequence databases forced us to use software that provides statistical estimates for the inference of sequence variations and post-translational modifications in known protein entries to match top-down MS data [50, 51]. The benefit of using species-specific transcriptomic databases to characterise or revise venom proteomes, as we have done in this study, allows the identification of unexplained mass discrepancies. This is exemplified in Fig. 6. The top-down MS/MS fragmentation pattern of the monoisotopic 6^+ topoisomer ion of *D. viridis* at m/z 1127.55 was assigned by TopPIC to a unknown proteoform of short neurotoxin S5C10 from *D. j. kaimosae* [P01419] (p-value of $9.15e^{-20}$), harbouring an unexplained mass discrepancy of +242.16 Da within the region encompassing residues 20-46 (Fig.6, upper panel). Searching against the *D. viridis* transcriptomic dataset, the same software identified protein T0913_Dv (Table S11) (p-value of $1.46e^{-31}$), which differs from *D. j. kaimosae* S5C10 at position 9 (D instead of N) and by having two additional residues (KI) at positions 50-51. These amino acid sequence variations explain exactly the mass difference of +242,16 Da (Fig. 6, lower panel).

Comparative compositional patterns

Broadly speaking, there is a good correlation between the transcriptomic and proteomic abundance of the major toxin families and their expression in the respective venom proteomes (compare Figs. 2 and 3). Both datasets show two clearly distinct overall toxin compositional patterns, with *D. polylepis* exhibiting a KUN-dominant transcriptome/venom proteome phenotype, in agreement with previous *D. polylepis* proteomic analyses [11], and all other mamba venoms (*D. angusticeps, D. viridis, D. j. jamesoni and D. j. kaimosae*) exhibiting 3FTx-dominant phenotypes and highly similar global toxin family compositons. However, the comparison of intact molecular masses across *Dendroaspis*, visualised in the Venn diagram displayed in Fig. 7A, illustrates the high variability between any two mamba venom proteomes. The identities and relative abundance of the major proteins within toxin classes with relative abundance ≥ 2% of the total ion current (TIC) vary between the four 3FTx-rich mamba venoms and between homologous venoms and transcriptomes (Fig. 4, Table 2). A notable discrepancy is that of the most abundantly transcribed toxin in *D. j. kaimosae,* a short neutrotoxin 1 (NTx-1)-like sequence (42% of total toxin transcriptome), which represents only 8.3% of the venom proteome. Similarly, *D. viridis* NTx-1 and *D. j. jamesoni* S2C4 accounted, respectively, for 5.6% and 36.4% of the toxin transcripts but only for 0.9% and 0.2% of the homologous venom proteomes. On the contrary, toxins C10S2C2 and muscarinic toxin MT2, medium-abundant 3FTx transcripts of the *D. angusticeps* transcriptome, were not found in the homologous venom proteomes (Table 2).

Notwithstanding apparent compositional discrepancies, and in accordance with the phylogenetic reconstruction of the genus (Fig. 2), PCA (Fig. 7B) clearly showed that the venoms of the *D. viridis*/*D. jamesoni* clade are more similar to each other than either are to the venoms of *D. polylepis* and *D. angusticeps*. PC1, PC2 and PC3 loadings explain,

respectively, 47.57%, 20.41% and 17.02% of the variability of *Dendroaspis* venoms. PC1 mainly differentiated *D. angusticeps* and *D. polylepis* from the *D. viridis, D. j. jamesoni* and *D. j. kaimosae* venoms by their relative abundance of short-chain orphan group XI 3FTx S5C4 [P01406] isoforms (molecular masses 6883.19 Da [*D. j. jamesoni*, Table S2], 6766.15 Da [*D. J. kaimosae*, Table S3] and 6775.20 Da [*D. viridis*, Table S4]). PC2 further discriminated venoms by their relative abundance of short-chain orphan group XI 3FTx DaF8 [P01404] (6594.16 Da, Table S5), 3FTx acetylcholinesterase inhibitor fasciculin 2 [P0C1Z0] (6746.01 Da, Table S5), short-chain orphan group X 3FTx C13S1C1 [P18329] (6630.28 Da, Table S3) and muscarinic rho-elapidotoxin Dp1a [P18329] (7303.4 Da, Table S5). PC3 loadings separated venoms per their relative abundance of voltage-gated potassium channel impairing Dendrotoxin-I□ □P00979□ (7128.52 Da, Table S6).

Venom Lethality and correlation with proteomes

Black mamba venom presents the greatest medical threat as revealed by venom LD_{50} data from murine studies (LD_{50} 6.2 µg/mouse; 0.33 µg/g) (Table 3). Despite being closely related to *D. j. jamesoni* and having an overall venom compositon similar to that of both *D. j. jamesoni* and *D. viridis* (Fig.3), *D. j. kaimosae* venom is generally twice as potent (mean i.v. LD_{50} 10.1 µg/mouse; 0.53 µg/g) than those of *D. j. jamesoni* and *D. viridis* (mean LD_{50}s 22.8 µg/mouse (1.2 µg/g), and 21.63 µg/mouse (1.14 µg/g), respectively) in the murine model. The dominant toxin in these three mambas, occurring in similar abundances (40.1% to 44.6% total venom proteomes), is SC54 [P01406] [43] (Table 2). Previously, S5C4 has been determined to be of low toxicitiy (LD_{50} >250 µg/g) [43] and therefore the striking differences in toxicity are unlikely to be due solely to S5C4. The possibility that S5C4 acts synergistically with other

toxins, as has been documented for *Dendroaspis* toxins [12, 44], deserves detailed pharmacological investigations. On the other hand, the greater abundance of the highly potent neurotoxin-1 (LD_{50} ~ 0.04–0.11 μg/g) [11, 52] in *D. j. kaimosae* (8.3%) compared to *D. j. jamesoni* (3.5%) and *D. viridis* (0.9%) venoms may contribute to these differences. Furthermore, the absence of neurotoxin-1 from *D. angusticeps* venom (Fig.3), and the abundance (29.4%) of 3FTx DaF8 (Table 2), which exhibited a low LD_{50} (20 μg/g mouse irrespective of the route of injection) compared to 2.2 μg per g mouse for whole venom [53], may explain why *D. angusticeps* venom exhibits the lowest toxicity (LD_{50} 37.9 μg/mouse; 1.99 μg/g) amongst mamba venoms in the murine model. The most potent venom is that of the most divergent *Dendroaspis* venom, that of the black mamba (*D. polylepis*) (Fig.3). This KUN-rich venom imparts a mean i.v. LD_{50} of 6.17 μg/mouse (0.33 μg/g). Whilst individual KUN toxins have been demonstrated to be measurably lower in toxicity than 3FTxs [11], we hypothesise that it is the combined effects of individual toxins that causes a synergistic increase in toxicity.

Genus-wide antivenomics

Immunoaffinity chromatography-based antivenomics [39] was employed to assess the immunological profile of the five *Dendroaspis* venoms against a panel of seven commercial antivenoms generated using immunisation mixtures that included one or more mamba venoms (Table 1) and two additional control antivenoms with no anticipated immunoreactivity against *Dendroaspis* venoms: Costa Rican EchiTAb-Plus-ICP® (anti-*Echis ocellatus*, *Bitis arietans*, and *Naja nigricollis*, all from Nigeria) [54-56] and UK EchiTAbG® (monospecific anti-*Echis ocellatus*, Nigeria) [54, 57] antivenom. The poor resolution of the chromatogram section containing 3FTx and KUN did not allow separation of these individual *Dendroaspis* venom

components. As these toxins dominate venom composition (Fig. 2 and 3) and toxicity [11, 12], the capability of the seven antivenoms marketed for the clinical treatment of *Dendroaspis* envenomings (Table 2) to reduce the total chromatographic area of the 3FTx/KUN section (7-16 min of elution time) was taken as a proxy for comparing their antivenomics effectiveness. Fig. 8 displays a summary of the global immunocapturing capability of the seven specific antivenom affinity chromatography columns against the venoms of the five mambas. Control columns (immobilised EchiTAb-Plus-ICP® and EchiTAbG® antivenoms, control equine IgGs, and mock matrix) retained 6-17% of venom components, thus limiting experimental noise. Based on their antivenomics profile, specific antivenoms can be grossly classified into three functional groups: a relatively ineffective group, including both VINS antivenoms; a modestly effective group comprising SAIMR polyvalent and Inoserp Panafricain™ antivenoms; and a highly effective group of immunodepleting antivenoms, comprising of Premium Serums Pan Africa, Sanofi-Pasteur FAV Afrique, and Bioclon's Antivipmyn®.

DISCUSSION

We have recently applied top-down venomics to detail the complexity of the venoms of the black mamba, *D. polylepis*, and the eastern green mamba, *D. angusticeps* [13]. This comparative work complemented previous peptide-centric venomic and toxicovenomic studies of green and black mamba venoms [11, 12]. In addition, it provided a proteoform-centric view of the venom proteomes of these medically important snakes, laying the foundations for rationalising the notably different potency of their venoms at locus resolution. Here we have extended the top-down analysis to the characterisation of venoms of the other species and subspecies of the genus *Dendroaspis*,

namely the Jameson's mamba (*D. j. jamesoni*), eastern or black-tailed Jameson's mamba (*D. j. kaimosae*) and the West African green mamba (*D. viridis*). Additionally, generation of venom-gland transcriptomes for the five congeners allowed a re-appraisal of the *D. polylepis* and *D. angusticeps* top-down assignments [13] made previously using a restricted *Dendroaspis*, NCBI-derived, reference database (comprising of 29 *D. angusticeps*, 20 *D. polylepis*, 8 *D. j. jamesoni*, 6 *D. viridis* and 1 *D. j. kaimosaei* non-redundant protein sequences). Application of the venom-gland transcriptomic data allowed the identification of an additional 23 (*D. angusticeps*), 29 (*D. polylepis*), 21 (*D. j. kaimosae*), 40 (*D. viridis*) and 25 (*D. j. jamesoni*) novel toxin sequences to the non-redundant full-length *Dendroaspis* sequence database (Supplementary Table S13), whilst confirming previously assigned venom components with increased confidence.

For the majority of these venoms, there was reasonable agreement between transcription and protein expression levels, as inferred from the venom gland transcriptomes and venom proteomes. The exception was that of *D. j. kaimosae*, the transcriptome of which was dominated by α-NTx 1 (43% total toxin expression) whereas 3FTx S5C4 was the most abundant protein (44.6% total proteome), matching historical investigations. Using capillary electrophoresis coupled to electrospray ionisation (ESI) and selected ion-monitoring mass-spectrometric (SlM-MS) detection, Perkins and Tomer [58] detected 83 peptides in the *D. j. kaimosae* venom. In concordance with our data, toxin S5C4 [P01406] was identified as the toxin with the highest relative ion abundance. Differences in venom-gland transcriptomes and proteins detected in venoms have been observed previously [26, 59]. For example, the most abundant toxin transcript in the venom-gland transcriptome of *B. arietans*, was not detected by proteomics. Reasons for these discrepancies have been postulated to include: i) transient/individual/temporal expression patterns of mRNA expression; ii) post-genomic

regulation [60], including miRNA-mediated posttranscriptional modulation of mRNA translation [61]; iii) a "hidden repertoire" of readily translatable transcripts for functional venom adaptation; and iv) methodological or statistical issues [62, 63]. On the other hand, the masses detected in mamba venom proteomes that could not be matched to homologous venom gland transcripts (Tables S7-S11) may be attributed to the fact that transcriptomic datasets were gathered from venom glands dissected from single specimens, whereas the top-down MS data were acquired from venoms pooled from wild-caught specimens. These details should be taken into account when comparing the proteome and transcriptome figures displayed in Table 2.

PLA_2 toxins are major components of elapid venoms [64-67], including African cobras [55, 68]. Despite this, no PLA_2 transcripts or toxins were detected in the venom gland transcriptomes or venom proteomes of *D. angusticeps* or *D. polylepis.* Furthermore, only a single PLA_2 of low abundance was detected in *D. viridis* (0.2% total venom proteome), *D. j. jamesoni* (2.2%) and *D. j. kaimosae* (1.8%). Fluorescent enzymatic PLA_2 assays further demonstrated negligible PLA_2 activity amongst the five mamba venoms (Fig. 5) and were in agreement with previous reports of low PLA_2 activity [11, 23]. Notably, the low-level PLA_2 detected is not a typical elapid group I PLA_2 [49], but a group IIE PLA_2, which to date has only been identified in venom gland transcriptomes of the non-elapid snakes *Atractaspis aterrima*, *Leioheterodon madagascarensis*, and *Dispholidus typus* [48]. The evolutionary pressures leading to the apparent complete loss of group I PLA_2 toxins and the unusual presence of group IIE amongst members of *Dendroaspis* deserves further investigation.

This study confirms the conclusions of previous investigations that the major *D. polylepis* venom components are KUN family toxins [11, 13]. Mapping the results of our genus-wide venomic analysis onto the phylogeny of the mambas (Fig. 2) also demonstrates

that the venom composition of *D. polylepis* is markedly distinct, and uniquely derived among Old World elapids, including the more typical, relatively conserved, 3FTx-dominated venoms of its congeners (*D. viridis, D. angusticeps, D. j. jamesoni* and *D. j. kaimosae*). As venom evolution is likely driven at least to some extent by dietary pressures [69-73], the divergent terrestrial ecology of *D. polylepis* compared to the arboreal niche occupied by all other mambas makes it plausible that this major difference in venom composition maybe due to dietary variation. Studies on the diets of wild mambas are scarce, although they are known to specialise primarily in warm-blooded prey. Birds and predominately terrestrial rodents make up similar proportions of the diet of *D. angusticeps* [74], whereas the diet of adult *D. jamesoni* is dominated by arboreal fauna, mainly birds, while terrestrial rodents are uncommon [7]. In contrast, *D. polylepis* is unique among mambas both in its venom composition and its terrestrial ecology, and also among Old World elapids, as its diet consists primarily of small mammals, rodents, hyrax, bushbabies, and bats [74-76]. Given the potential risk of injury posed by mammals to snakes, it seems reasonable to suppose a causal relation between these particularities: the unique diet of the black mamba may have resulted in a uniquely derived venom composition. The foraging strategy of the black mamba thus parallels that of the terrestrial Australian taipans (genus *Oxyuranus*), which are also mammal specialists and use large amounts of highly toxic venom in conjunction with a strike-release predatory strategy [77].

Our analysis of *Dendroaspsis* venom proteomes demostrates that the most abundant toxins in all five venoms are those previously assessed to be of relatively low toxicitiy (*D. angusticeps* DaF8 (29.4% total venom proteome) LD_{50} >100 µg/g mouse s.c., *D. viridis, D. j. jamesoni* and *D. j. kaimosae* S5C4 (40.1% to 44.6%) LD_{50} >250 µg/g mouse and *D. polylepis* dendrotoxins I (LD_{50} 38 µg/g) and K (LD_{50} 15 µg/g) [78]. However, it is relevant to note that

the major toxins of the black mamba, dendrotoxin-I (DTX-I) and dendrotoxin-K (DTX-K) have been shown to specifically target voltage-sensitive potassium channels in motor neurons with affinities in the nanomolar range [79]. These are present in large quantities (DTX-I, 24%; DTX-K, 7%) in black mamba venom (Table 2). In comparison, the similarly effective α-DTX in *D. angusticeps* [P00980] [80] is present in much smaller amounts (3.2% of the venom proteome, Table S8). On the other hand, whereas the major venom 3FTxs of *D. angusticeps, D. viridis*, *D. j. jamesoni* and *D. j. kaimosae* exhibit relatively high LD_{50}s in mice, e.g. DaF8 (LD_{50} >100 μg/g), S5C4 (LD_{50} >250 μg/g), S4C8 (LD_{50} 13.7 μg/g), S6C6 (LD_{50} 10 μg/g), S5C10 (LD_{50} 5.5 μg/g), or C13S1C1 (LD_{50} 40 μg/g) [44, 81], those present in black mamba venom (rho-elapidotoxin Dv2a, LD_{50} 0.045-0.08 μg/g mouse and α-NTX-1; LD_{50} 0.09 μg/g) are among the most potent toxins found in snake venoms [52, 82] and are heavily represented in its venom (Table 2). These short-chain 3FTxs target nicotinic acetylcholine receptors in the postsynaptic membrane of skeletal muscles, thereby impairing neuromuscular transmission. Together, DTXs I and K and 3FTxs Dv2a and α-NTX-1 comprise 46% of black mamba venom, and therefore they may be largely responsible for the great potency of *D. polylepis* venom in mammals. We hypothesise that this potency may be a result of selection, to rapidly incapacitate potentially dangerous mammalian prey. Further work testing the effects of different mamba venoms on natural prey species would be necessary to test this hypothesis and expand our understanding of the functional consequences of the variation in venom composition in the genus.

Synergistic action between proteins of low toxicity has also been established for proteins isolated from *D. angusticeps*, *D. polylepis* and *D. j. kaimosae* [11, 44, 53, 83-85]. In particular, a mixture of the *D. angusticeps* FS2 and dendrotoxin I venom KUN proteins showed a marked increase in toxicity, surpassing that of the individual proteins [86]. In

addition, a recent toxicovenomic analysis of *D. angusticeps* venom [12] revealed that, except for a single RP-HPLC fraction containing rho-elapitoxin-Da1b, thrombostatin, and fasciculin-2 (which exhibited an LD_{50} of 0.58 μg/g mouse), all other fractions lacked lethal activity at the doses tested. These observations are consistent with the view that the major, weakly toxic, components of mamba venoms may act synergistically. Toxin complexes often demonstrate novel activities that are completely absent from isolated subunits [87]. Analogously to *Dendroaspis*, the Texas coral snake (*Micrurus tener*) toxin MitTx is a heterodimeric complex consisting of a Kunitz-like subunit (MitTx-α) non-covalently linked to a catalytically-inactive PLA_2 homolog (MitTx-β) [88, 89]. This complex is able to activate ASIC1 somatosensory neuronal receptors to induce pain, but the individual subunits have no apparent functional effects on their own [88]. Whether *Dendroaspis* dendrotoxins form similar non-covalent functional complexes deserves a thorough investigation.

The pattern of intrageneric venom variability across *Dendroaspis* represented a valuable opportunity to investigate its potential implications for the treatment of snakebite victims with antivenoms available in sub-Saharan Africa. To this end, we applied antivenomics [39] to assess the immunological profile of the five *Dendroaspis* taxa against the seven commercial *Dendroaspis* antivenoms currently used in sub-Saharan Africa (Table 1) and two species-inappropriate commercial antivenoms (viper and cobra specific EchiTAb-Plus-ICP® and saw-scaled viper-specific EchiTAbG®) as controls (Fig. 8). Our results are in agreement with the conclusions of recent toxicovenomic studies comparing the efficiency of three commercial antivenoms to neutralise lethality in mice induced by *D. polylepis* and *D. angusticeps* venoms [11, 12]. In these studies, VINS African, VINS Central Africa and SAIMR polyvalent antivenoms were effective in the neutralisation of *D. polylepis* venom lethality, albeit at different ED_{50} (mg venom neutralised per mL antivenom): (0.76 mg/mL for

VINS African, 0.97 mg/mL for VINS Central Africa and 5.26 mg/mL for the SAIMR polyvalent antivenom) [11, 90]. The SAIMR and VINS African antivenoms displayed neutralising ability against the lethal effect of *D. angusticeps* venom (i.v. LD_{50} of 1.3 μg/g mouse), with ED_{50}s of 4.0 mg/mL and 2.4 mg/mL, respectively. However, the VINS Central African antivenom failed to neutralise the lethality of *D. angusticeps* venom at the lowest venom/antivenom ratio tested (1.0 mg venom/mL antivenom) [11]. In the context of the venom proteomes generated in this study, and the notable differences in venom composition between *D. polylepis* and *D. angusticeps*, the inability of VINS Central African to neutralise *D. angusticeps* venom in the previous study is not suprising, as this antivenom was manufactured using only *D. polylepis* venom. VINS Central African antivenom is currently available for purchase in regions of Africa where more than one species of *Dendroaspsis* is present. Furthermore, our results complement a recent peptide microarray analysis of the immunoreactivity of VINS African, VINS Central Africa and SAIMR polyvalent antivenoms, which demonstrated that both VINS products have weak immuno-reactivity against *Dendroaspis* toxins [90].

Comparing the levels of immune recognition gathered from antivenomics with the *in vivo* neutralisation capacity of an antivenom is not straightforward, since both experiments involve radically different protocols. Nonetheless, a variety of antivenomics studies conducted on a number of viperid venoms have indicated that a moderate immunocapturing capability of ~20%–25% correlated with a positive outcome in *in vivo* neutralisation tests (reviewed in [91]). In view of these results, this estimate does not seem to be valid for mamba venoms, where the immunocapture ability of therapeutic antivenoms should be considered ≥50%. As a result of this work we now have a comprehensive, genus-wide, overview of the

immune cross-reactivity profile of a panel of commercial antivenoms towards the venoms of medically important *Dendroaspsis*.

CONCLUDING REMARKS

To the best of our knowledge, this study represents the first genus-wide transcriptomic and proteomic analysis of venom composition across *Dendroaspis*. The information gathered enables us to rationalise the diverse pharmacological profiles of mamba venoms at locus resolution. Additionally, this understanding will contribute to the selection and design of key toxin immunogens [90, 92-94], with a view to generating safer and more efficacious antivenom, capable of neutralising envenomations caused by any mamba species. Toxins bearing the highest prey incapacitation activity are often also the most medically important molecules in the context of a human envenoming. Therefore, although the possibility that different toxins act synergistically should not be ruled out *a priori*, insights into the selective pressures that resulted in local adaptation and species-level divergence in venoms can shed light on the mutually enlightening relationship between evolutionary and clinical toxinology. Identifying the molecular basis of venomous snake predator-prey relations may assist in the identification of toxins that most need to be neutralized to reverse the effects of venom, thereby guiding the rational development of future snakebite therapeutics. Devising effective, affordable and safe antivenoms represents a priority for reducing the mortality, morbidity and socioeconomic burden of tropical snakebite [94, 95]. Genus-wide antivenomics represents a powerful tool for this purpose. In addition to snakebites caused by accidental encounters between snakes and humans in their shared natural habitat, non-native snakes, including mamba species, maintaned in captivity as pets or in zoological exhibitions can be a

problematic source of envenomation worldwide [96-98]. For some cases, this genus-wide overview of the antivenomics profiles of available antivenoms may help in improving the clinical management of snakebite by both wild and captive exotic animals.

DATA ACCESSIBILITY

Transcriptomic data have been submitted to the NCBI Sequence Read Archive (https://www.ncbi.nlm.nih.gov/sra) (numbers SAMN06324384, SAMN06324385, SAMN06324386, SAMN06324387, SAMN06324388). The top-down MS datasets have been submitted to ProteomeXchange [99] via the MaSSIVE repository (http://massive.ucsd.edu/) with accession number MSV000080491. Mitochondrial gene sequence data used to build the phylogeny are accessible as GenBank (https://www.ncbi.nlm.nih.gov/genbank/) accession numbers MF407265-MF407274.

ACKNOWLEDGEMENTS

This study was supported by grants BFU2013-42833-P (Ministerio de Economía y Competitividad, Madrid, Spain), MR/L01839X/1 (Medical Research Council, UK), NNF13OC0005613 (the Novo Nordisk Foundation), Knud Højgaards Fond, Augustinusfonden, PE 2600/1 and the Cluster of Excellence UniCat (Deutsche Forschungsgemeinschaft, Bonn, Germany).

REFERENCES

1. JP Chippaux, A Diouf, A Massougbodji, RP Stock, O Kane, AM Dièye, A Lam Faye, M Mbaye Sène, HJ Parra, Report of the 4th International Conference on Envenomations by Snakebites and Scorpion Stings in Africa, Dakar, April 25-29, 2011. Bull. Soc. Pathol. Exot. 2012; 105:194-8.
2. AG Habib, A Kuznik, M Hamza, MI Abdullahi, BA Chedi, JP Chippaux, DA Warrell, Snakebite is under appreciated: Appraisal of burden from West Africa. PLoS Negl. Trop. Dis. 2015; 9:e0004088.
3. S Spawls, B. Branch, The Dangerous Snakes of Africa. Southern Book Publishers, London, 1995.
4. M O'Shea, Venomous Snakes of the World. Princeton University Press, 2011. ISBN 10: 0691150230.
5. A Loveridge, New tree snakes of the genera *Thrasops* and *Dendraspis* from Kenya Colony. Proc. Biol. Soc. Washington 1936; 49:63-6.
6. MJ Angilletta, Sedentary behaviors by Green Mambas *Dendroaspis angusticeps*. Herpetol. Natl. History 1994; 2:105-11.
7. L Luiselli, FM Angelici, GC Akani, Large elapids and arboreality: the ecology of Jameson's green mamba (*Dendroaspis jamesoni*) in an Afrotropical forested region. Contributions to Zoology 2000; 69:147-55.
8. DA Warrell, Clinical toxicology of snakebite in Africa and the Middle East/Arabian peninsula. *Handbook of clinical toxicology of animal venoms and poisons* (Meier, J., White, J, eds.), CRC Press, Inc., 1995; p. 433-492.

9. PS Hodgson, TM Davidson, Biology and treatment of the mamba snakebite. Wilderness Environ. Med. 1996; 7:133-45.

10. J-P Chippaux, Snake Venoms and Envenomations. Krieger Publishing Company, United States, 2006. ISBN 978-1-57524-272-9.

11. AH Laustsen, B Lomonte, B Lohse, J Fernández, JM Gutiérrez, Unveiling the nature of black mamba (*Dendroaspis polylepis*) venom through venomics and antivenom immunoprofiling: Identification of key toxin targets for antivenom development. J. Proteomics 2015; 119:126-42.

12. LP Lauridsen, AH Laustsen, B Lomonte, JM Gutiérrez, Toxicovenomics and antivenom profiling of the Eastern green mamba snake (*Dendroaspis angusticeps*). J. Proteomics 2016; 136:248-61.

13. D Petras, P Heiss, RA Harrison, RD Süssmuth, JJ Calvete, Top-down venomics of the East African green mamba, *Dendroaspis angusticeps*, and the black mamba, *Dendroaspis polylepis*, highlight the complexity of their toxin arsenals. J. Proteomics 2016; 146:148-64.

14. E Karlsson, PM Mbugua, D Rodríguez-Iturralde, Fasciculins, anticholinesterase toxins from the venom of the green mamba *Dendroaspis angusticeps*. J. Physiol. Paris 1984; 79:232-40.

15. O Yasuda, S Morimoto, Y Chen, B Jiang, T Kimura, S Sakakibara, E Koh, K Fukuo, S Kitano, T Ogihara, Calciseptine binding to a 1,4-dihydropyridine recognition site of the L-type calcium channel of rat synaptosomal membranes. Biochem. Biophys. Res. Commun. 1993; 194:587-94.

16. RM Kini, R Doley, Structure, function and evolution of three-finger toxins: mini proteins with multiple targets. Toxicon 2010; 56:855-67.

17. D Servent, G Blanchet, G Mourier, C Marquer, E Marcon, C Fruchart-Gaillard, Muscarinic toxins. Toxicon 2011; 58:455-63.

18. AL Harvey, Twenty years of dendrotoxins. Toxicon 2001; 39:15-26.

19. AL Harvey, B Robertson, Dendrotoxins: structure-activity relationships and effects on potassium ion channels. Curr. Med. Chem. 2004; 11:3065-72.

20. Schweitz, C Heurteaux, P Bois, D Moinier, G Romey, M Lazdunski, Calcicludine, a venom peptide of the Kunitz-type protease inhibitor family, is a potent blocker of high-threshold Ca^{2+} channels with a high affinity for L-type channels in cerebellar granule neurons. Proc. Natl. Acad. Sci. USA 1994; 91:878-82.

21. SA Park, TG Kim, MK Han, KC Ha, SZ Kim, YG Kwak, Dendroaspis natriuretic peptide regulates the cardiac L-type Ca^{2+} channel activity by the phosphorylation of α1c proteins. Exp. Mol. Med. 2012; 44:363-8.

22 H Schweitz, P Pacaud, S Diochot, D Moinier, M Lazdunski, MIT1, a black mamba toxin with a new and highly potent activity on intestinal contraction. FEBS Lett. 1999; 461:183-8.

23 SA Ibrahim, ARM Masr, Action of phospholipase A from black mamba (*Dendroaspis polylepis*) venom on phospholipids of human blood. Toxicon 1975; 13:99.

24. S Eichberg, L Sanz, JJ Calvete, D Pla, Constructing comprehensive venom proteome reference maps for integrative venomics. Expert Rev. Proteomics 2015; 12:557-73.

25. D Petras, P Heiss, RD Süssmuth, JJ Calvete, Venom Proteomics of Indonesian King Cobra, *Ophiophagus hannah*: Integrating Top-Down and Bottom-Up Approaches. J. Proteome Res. 2015; 14:2539-56.

26. SC Wagstaff, L Sanz, P Juárez, RA Harrison, JJ Calvete, Combined snake venomics and venom gland transcriptomic analysis of the ocellated carpet viper, *Echis ocellatus*. J. Proteomics. 2009; 71:609-23.

27. RK Brahma, RJ McCleary, RM Kini, R Doley, Venom gland transcriptomics for identifying, cataloging, and characterizing venom proteins in snakes. Toxicon 2015; 93:1-10

28. SC Wagstaff, RA Harrison, Venom gland EST analysis of the saw-scaled viper, *Echis ocellatus*, reveals novel α9β1 integrin-binding motifs in venom metalloproteinases and a new group of putative toxins, renin-like aspartic proteases. Gene 2006; 377:21-32.

29. NR Casewell, RA Harrison, W Wüster, SC Wagstaff SC, Comparative venom gland transcriptome surveys of the saw-scaled vipers (Viperidae: *Echis*) reveal substantial intra-family gene diversity and novel venom transcripts. BMC Genomics 2009; 10:564.

30. D Pla, L Sanz, G Whiteley, SC Wagstaff, RA Harrison, NR Casewell, JJ Calvete, What killed Karl Patterson Schmidt? Combined venom gland transcriptomic, venomic and antivenomic analysis of the South African green tree snake (the boomslang), *Dispholidus typus*. Biochim. Biophys. Acta (General Subjects) 2017; 1861:814-23.

31. J Archer, G Whiteley, NR Casewell, RA Harrison, SC Wagstaff, VTBuilder: a tool for the assembly of multi isoform transcriptomes. BMC bioinformatics 2014; 15:389.

32. S Goetz, JM Garcia-Gomez, J Terol, TD Williams, SH Nagaraj, MJ Nueda, M Robles, M Talon, J Dopazo, A Conesa, High-throughput functional annotation and data mining with the Blast2GO suite. Nucleic Acids Res. 2008, 36, 3420–35.

33. HT Heberle, GV Meirelles, FR da Silva, GP Telles, R Minghim, InteractiVenn: a web-based tool for the analysis of sets through Venn diagrams. BMC Bioinformatics 2015; 16:169.

34. JAA Nylander, MrModeltest v2, 2004. Program distributed by the author. Evolutionary Biology Centre, Uppsala University, Uppsala.

35. F Ronquist, M Teslenko, P van der Mark, DL Ayres, A Darling, S Höhna, B Larget, L Liu, MA Suchard, JP Huelsenbeck, Mrbayes 3.2: Efficient Bayesian phylogenetic inference and model choice across a large model space. Systematic Biology 2012; 61:539-42.

36. Y Zheng, JJ Wiens, Combining phylogenomic and supermatrix approaches, and a time-calibrated phylogeny for squamate reptiles (lizards and snakes) based on 52 genes and 4162 species. Mol. Phylogenet. Evol. 2016; 94:537–47.

37. MSY Lee, KL Sanders, B King, A Palci, A. Diversification rates and phenotypic evolution in venomous snakes (Elapidae). Royal Society Open Science 2016; 3: 150277. http://dx.doi.org/10.1098/rsos.150277

38. World Health Organization. WHO Guidelines for the Production, Control and Regulation of Snake Antivenom Immunoglobulins. World Health Organization, Geneva, 2016. http://www.who.int/bloodproducts/snake_antivenoms/snakeantivenomguide/en/

39. D Pla, JM Gutiérrez, JJ Calvete, Second generation snake antivenomics. Comparing immunoaffinity and immunodepletion protocols. Toxicon 2012; 60: 688-99.

40. GC Howard, MR Kaser, Making and Using Antibodies: A Practical Handbook, Second Edition. CRC Press, Taylor & Francis Group, Boca Raton (FL) 2013; 458 pp. ISBN 9781439869086

41. MJ Margres, K Aronow, J Loyacano, DR Rokyta, The venom-gland transcriptome of the eastern coral snake (*Micrurus fulvius*) reveals high venom complexity in the intragenomic evolution of venoms. BMC Genomics 2013; 14:531.

42. F Ducancel, EG Rowan, E Cassar, AL Harvey, A Menez, JC Boulain, Amino acid sequence of a muscarinic toxin deduced from the cDNA nucleotide sequence. Toxicon 1991; 29:516-520.

43. FJ Joubert, AJ Strydom, N Taljaard, Snake venoms. The amino-acid sequence of protein S5C4 from *Dendroaspis jamesoni kaimosae* (Jameson's mamba) venom. Hoppe-Seyler's Z. Physiol. Chem. 1978; 359:741-9.

44. FJ Joubert, N Taljaard, The amino-acid sequence of protein S2C4 from *Dendroaspis jamesoni kaimosae* (Jameson's mamba) venom. Hoppe-Seyler's Z. Physiol. Chem. 1979; 360:571-80.

45. AJ Strydom, Snake venom toxins. The amino acid sequences of two toxins from *Dendroaspis jamesoni kaimosae* (Jameson's mamba) venom. Biochim. Biophys. Acta 1973; 328:491-509.

46. ST Chatrath, A Chapeaurouge, Q Lin, TK Lim, N Dunstan, P Mirtschin, PP Kumar, RM Kini, Identification of novel proteins from the venom of a cryptic snake *Drysdalia coronoides* by a combined transcriptomics and proteomics approach. J. Proteome Res. 2011; 10:739-50.

47. FJ Joubert, CC Viljoen, Snake venom. The amino-acid sequence of the subunits of two reduced and S-carboxymethylated proteins (C8S2 and C9S3) from *Dendroaspis angusticeps* venom. Hoppe-Seyler's Z. Physiol. Chem. 1979; 360:1075-1090.

48. BG Fry, H Scheib, ILM Junqueira-de-Azevedo, DA Silva, NR Casewell, Novel transcripts in the maxillary venom glands of advanced snakes. Toxicon 2012; 59:696-708.

49. K Sunagar, T Jackson, T Reeks, BG Fry, Group I phospholipase A_2 enzymes. Venomous Reptiles and Their Toxins: Evolution, Pathophysiology and

Biodiscovery (BG Fry, editor), Oxford University Press, Oxford, 2015; 327-34. ISBN 9780199309399.

50. W Cai, H Guner, ZR Gregorich, AJ Chen, S Ayaz-Guner, Y Peng, SG Valeja, X Liu, Y Ge, MASH Suite Pro: A Comprehensive Software Tool for Top-down Proteomics. Mol. Cell. Proteomics 2016; 15:703-14.

51. Q Kou, L Xun, X Liu, TopPIC: a software tool for top-down mass spectrometry-based proteoform identification and characterization. Bioinformatics. 2016; 32:3495-7.

52. DJ Strydom, Snake venom toxins. The amino-acid sequence of two toxins from *Dendroaspis polylepis polylepis* (black mamba) venom. J. Biol. Chem. 1972; 247:4029–42.

53. CC Viljoen, DP Botes, Snake venom toxins. The purification and amino acid sequence of toxin TA2 from *Dendroaspis angusticeps* venom. J. Biol. Chem. 1974; 249:366-372.

54. SB Abubakar, IS Abubakar, AG Habib, A Nasidi, N Durfa, PO Yusuf, S Larnyang, J Garnvwa, E Sokomba, L Salako, GD Laing, RD Theakston, E Juszczak, N Alder, DAWarrell, Nigeria-UK EchiTab Study Group, Pre-clinical and preliminary dose-finding and safety studies to identify candidate antivenoms for treatment of envenoming by saw-scaled or carpet vipers (*Echis ocellatus*) in northern Nigeria. Toxicon 2010; 55:719-23.

55. D Petras, L Sanz, A Segura, M Herrera, M Villalta, D Solano, M Vargas, G León, DA Warrell, RD Theakston, RA Harrison, N Durfa, A Nasidi, JM Gutiérrez, JJ Calvete, Snake venomics of African spitting cobras: toxin composition and assessment of congeneric cross-reactivity of the pan-African EchiTAb-Plus-ICP antivenom by antivenomics and neutralization approaches. J. Proteome Res. 2011; 10:1266-80.

56. LV Sánchez, D Pla, M Herrera, J-P Chippaux, JJ Calvete, JM Gutiérrez, Evaluation of the preclinical efficacy of four antivenoms, distributed in sub-Saharan Africa, to neutralize the venom of the carpet viper, *Echis ocellatus*, from Mali, Cameroon, and Nigeria. Toxicon 2015; 106:97-107.

57. NR Casewell, DA Cook, SC Wagstaff, A Nasidi, N Durfa, W Wüster, RA Harrison, Pre-clinical assays predict pan-African Echis viper efficacy for a species-specific antivenom. PLoS Negl. Trop. Dis. 2010; 4:e851.

58. JR Perkins KB Tomer, Characterization of the lower-molecular-mass fraction of venoms from *Dendroaspis jamesoni kaimosae* and *Micrurus fulvius* using capillary electrophoresis electrospray mass spectrometry. Eur. J. Biochem. 1995; 233:815-27.

59. E Fasoli, L Sanz, SC Wagstaff, RA Harrison, PG Righetti, JJ Calvete, Exploring the venom proteome of the African puff adder, *Bitis arietans*, using a combinatorial peptide ligand library approach at different pHs. J. Proteomics 2010; 73:932-92.

60. NR Casewell, SC Wagstaff, W Wüster, DA Cook, FM Bolton, SI King, D Pla, L Sanz, JJ Calvete, RA Harrison, Medically important differences in snake venom composition are dictated by distinct postgenomic mechanisms. Proc. Natl. Acad. Sci. USA. 2014; 111:9205-10.

61. J Durban, A Pérez, L Sanz, A Gómez, F Bonilla, S Rodríguez, D Chacón, M Sasa, Y Angulo, JM Gutiérrez, JJ Calvete, Integrated "omics" profiling indicates that miRNAs are modulators of the ontogenetic venom composition shift in the Central American rattlesnake, *Crotalus simus simus*. BMC Genomics 2013; 14:234.

62. JJ Li, MD Biggin, Gene expression. Statistics requantitates the central dogma. Science 2015; 347:1066-7.

63. DR Rokyta, MJ Margres, K Calvin, Post-transcriptional Mechanisms Contribute Little to Phenotypic Variation in Snake Venoms. G3 2015; 5:2375-82.

64. VJ Lynch, Inventing an arsenal: adaptive evolution and neofunctionalization of snake venom phospholipase A_2 genes. BMC Evol. Biol. 2007; 7:2.

65. R Doley, X Zhou, RM Kini, Snake venom phospholipase A_2 enzymes, Handbook of Venoms and Toxins of Reptiles (SP Mackessy, editor), CRC Press, Taylor & Francis Group, Boca Raton, FL, 2010; 173-206. ISBN 978-0-8493-9165-1

66. TN Jackson, K Sunagar, UE Undheim, I Koludarov, AH Chan, K Sanders, SA Ali, I Hendrikx, N Dunstan, BG Fry, Venom down under: dynamic evolution of Australian elapid snake toxins. Toxins 2013; 5:2621-55.

67. B Lomonte, P Rey-Suárez, J Fernández, M Sasa, D Pla, N Vargas, M Bénard-Valle, L Sanz, C Corrêa-Netto, V Núñez, A Alape-Girón, A Alagón, JM Gutiérrez, JJ Calvete, Venoms of Micrurus coral snakes: Evolutionary trends in compositional patterns emerging from proteomic analyses. Toxicon 2016; 122:7-25.

68. LP Lauridsen, AH Laustsen, B Lomonte, JM Gutiérrez, Exploring the venom of the forest cobra snake: Toxicovenomics and antivenom profiling of *Naja melanoleuca*. J. Proteomics 2017; 150:98-108.

69. JC Daltry, W Wüster, RS Thorpe, Diet and snake venom evolution. Nature 1996; 379: 537-40.

70. NJ Da Silva, SD Aird, Prey specificity, comparative lethality and compositional differences of coral snake venoms. Comparat. Biochem. Physiol. Part C 2001; 128:425–56.

71. HL Gibbs, W Rossiter, Rapid evolution by positive selection and gene gain and loss: PLA_2 venom genes in closely related Sistrurus rattlesnakes with divergent diets. J. Mol. Evol. 2008; 66:151-66.

72. A Barlow, CE Pook, RA Harrison, W Wüster, Coevolution of diet and prey-specific venom activity supports the role of selection in snake venom evolution. Proc. Royal Soc. B 2009; 276: 2443–9.

73. ML Holding, DH Drabeck, SA Jansa, HL Gibbs, Venom Resistance as a Model for Understanding the Molecular Basis of Complex Coevolutionary Adaptations. Integr. Comp. Biol. 2016; 56:1032-43.

74. W Branch, G Haagner, R Shine, Is there an ontogenetic shift in mamba diet? Taxonomic confusion and dietary records for black and green mambas (*Dendroaspis*: Elapidae). Herpetol. Nat. Hist.1995; 3:171-8.

75. GV Haagner, DR Morgan, The maintenance and propagation of the Black mamba *Dendroaspis polylepis* at the Manyeleti Reptile Centre, Eastern Transvaal, Int. Zoo Yearbook 1993; 32:191–6.

76. Phelps, A study of the black mamba (*Dendroaspis polylepis*) in KwaZulu-Natal, South Africa, with particular reference to long-term refugia. Herpetol. Bull. 2002; 80: 7-19.

77. R Shine. J Covacevich, Ecology of highly venomous snakes: the Australian genus *Oxyuranus* (Elapidae). J. Herpetol 1983; 17: 60-69.

78. D Mebs, F Hucho, Toxins acting on ion channels and synapses, Handbook of Toxinology (WT Shier, D Mebs, eds.), Marcel Dekker, Inc., New York and Basel, 1990, 493-600. ISBN 0-8247-8374-3

79. B Robertson, D Owen, J Stow, C Butler, C Newland, Novel effects of dendrotoxin homologues on subtypes of mammalian Kv1 potassium channels expressed in *Xenopus oocytes*. *FEBS Lett.* 1996, *383*, 26–30.

80. S Grissmer, AN Nguyen, J Aiyar, DC Hanson, RJ Mather, GA Gutman, MJ Karmilowicz, DD Auperin, KG Chandy, Pharmacological characterization of five cloned voltage-gated K+ channels, types Kv1.1, 1.2, 1.3, 1.5, and 3.1, stably expressed in mammalian cell lines. Mol Pharmacol. 1994; 45:1227-34.

81. FJ Joubert, N Taljaard, The complete primary structures of two reduced and S carboxymethylated Angusticeps-type toxins from *Dendroaspis angusticeps* (green mamba) venom. Biochim. Biophys. Acta 1980; 623:449-56.

82. G Bechis, C Granier, J van Rietschoten, E Jover, H Rochat, F Miranda, Purification of six neurotoxins from the venom of *Dendroaspis viridis*. Primary structure of two long toxins. Eur. J. Biochem. 1976; 68:445-56.

83. DJ Strydom, DP Botes, Snake venom toxins. I. Preliminary studies on the separation of toxins of Elapidae venoms. Toxicon 1970; 8:203-209.

84. CC Viljoen, DP Botes, Snake venom toxins. The purification and amino acid sequence of toxin F VII from *Dendroaspis angusticeps* venom. J. Biol. Chem. 1973; 248:4915-9.

85. DJ Strydom, Snake Venom Toxins The amino-acid sequence of a short-neurotoxin homologue from *Dendroaspis polylepis polylepis* (Black Mamba) venom. Eur. J. Biochem. 1977; 76:99-106.

86. DJ Strydom, Snake venom toxins. Purification and properties of low-molecular-weight polypeptides of *Dendroaspis polylepis polylepis* (black mamba) venom. Eur. J. Biochem. 1976; 69:169-76.

87. CJ Böhlen, D Julius, Receptor-targeting mechanisms of pain-causing toxins: How ow? Toxicon 2012; 60:254-264.

88. CJ Böhlen, AT Chesler, R Sharif-Naeini, KF Medzihradszky, S Zhou, D King, EE Sánchez, AL Burlingame, AI Basbaum, DA Julius, heteromeric Texas coral snake toxin targets acid-sensing ion channels to produce pain. Nature 2011; 479:410-414.

89. I Baconguis, CJ Böhlen, A Goehring, D Julius, E Gouaux, X-ray structure of acid sensing ion channel 1-snake toxin complex reveals open state of a Na^+-selective channel. Cell 2014; 156:717-729.

90. M Engmark, MR Andersen, AH Laustsen, J Patel, E Sullivan, F de Masi, CS Hansen, JV Kringelum, B Lomonte, JM Gutiérrez, O Lund, High-throughput immuno-profiling of mamba (*Dendroaspis*) venom toxin epitopes using high-density peptide microarrays. Sci. Rep. 2016; 6:36629.

91. JJ Calvete, L Sanz, D Pla, B Lomonte, JM Gutiérrez, Omics meets biology: Application to the design and preclinical assessment of antivenoms. Toxin 2014; 6:3388-405.

92. RA Harrison, DA Cook, C Renjifo, NR Casewell, RB Currier, SC Wagstaff, Research strategies to improve snakebite treatment: challenges and progress. J. Proteomics 2011; 74:1768-80.

93. G Blanchet, D Alili, A Protte, G Upert, N Gilles, L Tepshi, EA Stura, G Mourier, D Servent, Ancestral protein resurrection and engineering opportunities of the mamba aminergic toxins. Sci Rep. 2017; 7:2701.

94. RA Harrison, JM Gutiérrez, Priority Actions and Progress to Substantially and Sustainably Reduce the Mortality, Morbidity and Socioeconomic Burden of Tropical Snakebite. Toxins 2016; 8:351.

95. DA Warrell, Snake bite. The Lancet 375 (2010) 77-88.

96. T Leclerc, B Debien, JP Perez, MP Petit, B Lenoir, Mamba envenomation in mainland France: management of exotic envenomations needs rethinking. Ann. Fr. Anesth. Reanim. 27 (2008) 323-5.

97. BJ Warrick, LV Boyer, SA Seifert, Non-native (exotic) snake envenomations in the U.S., 2005-2011. Toxins 6 (2014) 2899-911.

98. S de Rudnicki, B Debien, T Leclerc, P Clapson, A Merens, JP Perez, B Lenoir, Paraspecific antivenins and exotic bites of snakes: about two case reports. Ann. Fr. Anesth. Reanim. 27 (2008) 326-9.

99. JA Vizcaíno, EW Deutsch, R Wang, A Csordas, F Reisinger, D Ríos, JA Dianes, Z Sun, T Farrah, N Bandeira, PA Binz, I Xenarios, M Eisenacher, G Mayer, L Gatto, A Campos, RJ Chalkley, HJ Kraus, JP Albar, S Martinez-Bartolomé, R Apweiler, GS Omenn, L Martens, AR Jones, H Hermjakob, ProteomeXchange provides globally co ordinated proteomics data submission and dissemination. Nature Biotechnol. 2014; 30:223-26.

100. B Ramos-Cerrillo, AR de Roodt, J-P Chippaux, L Olguín, A Casasola, G Guzmán, J Paniagua-Solís, A Alagón, RP Stock, Characterization of a new polyvalent antivenom (Antivipmyn® Africa) against African vipers and elapids. Toxicon 2008; 52: 881-8.

Table 1. Characteristics of the antivenoms for sub-Saharan Africa used in the study.

Antivenom	Manufacturer	Venoms used in immunisation[a]		Production animal	Active substance
		Viperidae	Elapidae		
SAIMR polyvalent snake antivenom	South African Vaccine Producers	*Bitis arietans* *Bitis gabonica*	*Dendroaspis angusticeps* *Dendroaspis jamesoni* *Dendroaspis polylepis* *Haemachatus haemachatus* *Naja annulifera* *Naja melanoleuca* *Naja mossambica* *Naja nivea*	Horse	$F(ab')_2$
FAV Afrique	Sanofi-Pasteur	*Bitis arietans* *Bitis gabonica* *Echis leucogaster* *Echis ocellatus*	*Dendroaspis jamesoni* *Dendroaspis polylepis* *Dendroaspis viridis* *Naja haje* *Naja nigricollis*	Horse	$F(ab')_2$
EchiTAb-Plus-ICP®	Instituto Clodomiro Picado	*Echis ocellatus* *Bitis arietans*	*Naja nigricollis*	Horse	IgG
Inoserp Panafricain™	Inosan Biopharma	*Bitis arietans* *Bitis gabonica* *Echis leucogaster* *Echis ocellatus* *Echis pyramidum*	*Dendroaspis jamesoni* *Dendroaspis polylepis* *Naja haje* *Naja melanoleuca* *Naja nigricollis* *Naja pallida*	Horse	$F(ab')_2$
Snake Antiserum	VINS Bioproducts	*Bitis gabonica*	*Dendroaspis polylepis*	Horse	$F(ab')_2$

(Central Africa)		*Echis carinatus* *Daboia russelli*			
Snake Antiserum (African)	VINS Bioproducts	*Bitis arietans* *Bitis gabonica* *Echis leucogaster* *Echis ocellatus*	*Dendroaspis jamesoni* *Dendroaspis polylepis* *Dendroaspis viridis* *Naja haje* *Naja melanoleuca* *Naja nigricollis*	Horse	$F(ab')_2$
Snake Antiserum (Pan Africa)	Premium Serum and Vaccines	*Bitis arietans* *Bitis gabonica* *Bitis nasicornis* *Bitis rhinoceros* *Echis carinatus* *Echis leucogaster* *Echis ocellatus*	*Dendroaspis angusticeps* *Dendroaspis jamesoni* *Dendroaspis polylepi* *Dendroaspis viridis* *Naja haje* *Naja melanoleuca* *Naja nigricollis*	Horse	$F(ab')_2$
Antivipmyn® Africa	Instituto Bioclon	*Bitis arietans* *Bitis gabonica* *Echis leucogaster* *Echis ocellatus* *Echis pyramidum*	*Dendroaspis polylepis* *Dendroaspis viridis* *Naja haje* *Naja melanoleuca* *Naja nigricollis* *Naja pallida*	Horse	$F(ab')_2$
EchiTAbG	Micropharm	*Echis ocellatus*		Sheep	IgG

[a] Information on the venoms used for immunisation for antivenoms VINS and Premium Serums and Vaccines was obtained from the table of venoms neutralised by the antivenoms in the inserts of the products. In the case of Antivipmyn® Africa, information was obtained from Ramos-Cerrillo et al. [100].

Table 2. Comparative overview of the number and relative abundance (% of venom protein TIC) of the major 3FTx and KUN proteoforms assigned by top-down MS in the venom proteomes (P) or gathered by venom gland transcriptomics (T) of *Dendroaspis viridis* (*Dv*), *D. jamesoni jamesoni* (*Djj*), *D. j. kaimosae* (*Djk*), *D. angusticeps* (*Da*), and *D. polylepis* (*Dp*).

	Dv		*Djj*		*Djk*		*Da*		*Dp*	
3FTx	P	T	P	T	P	T	P	T	P	T
nº proteoforms	34	47	27	22	33	14	80	22	61	23
% total toxinome	76.7	79.4	65.5	81.4	74.8	68.3	64.2	70.1	40.0	44.9
S5C4	40.1	20	45.5	27.8	44.6					
S6C6			8.7	3.1	3.5	5.4				
S2C4			0.2	36.4						
NTx-1	0.9	5.6	3.5	3.9	8.3	43.1			5.9	17.7
Mambin	2.1	0.6	3.4	2.7	1.6	4.1				
C13S1C1	5.4	3.5	1.1		15.1	1.3	5.6			

	C10S2C2							10.9		
	S4C8	7.7	12.1							
	S5C10	10.1	3.7							
	α-eTx Dv2a								8.9	11.7
	Mus Tx-1								6.3	1.5
	Mus Tx-2							9.5		
	rho-eTx Dp1a						6.5	2.2		
	Calciseptine					3.9			7.2	2.4
	DaF8						29.4	7.5		
Kun										
	nº proteoforms	14	13	16	6	6	5	25	7	38	11
	% total toxinome	5.6	14.1	16.3	15.3	9.6	14.1	15.5	16.1	39.0	48.7
	Dendro I			12.5	10.4	8.9		3.4		24.2	30.1
	Dendro K								3.1	7.2	7.3
	Toxin C13S2C3	2.1									

Fasciculin 2	4.9		12.5	23.1
Dendro B		8.5		

Table 3. The median murine lethal dose (LD_{50}) of mamba venoms determined by the intravenous route.

Venom	**Origin**	**µg / 18-20 g mouse (95% confidence interval)**	**µg / g (95% confidence interval)**
D. angusticeps	Tanzania	37.9 (30.6 – 46.7)	1.99 (1.61 – 2.46)
D. j. jamesoni	Cameroon	22.8 (12.3 – 39.1)	1.20 (0.65 – 2.06)
D. j. kaimosae	Uganda	10.1 (6.2 – 34.2)	0.53 (0.33 – 1.80)
D. polylepis	Tanzania	6.2 (3.1 – 10.2)	0.33 (0.16 – 0.54)
D. viridis	Togo	21.6 (15.2 – 25.8)	1.14 (0.80 – 1.36)

LEGENDS TO FIGURES

Figure 1. Distribution of *Dendroaspis* species in sub-Saharan Africa. A) Eastern green mamba (*D. angusticeps*), B) Jameson's mambas (*D. j. jamesoni* [pale blue] and *D. j. kaimosae* [dark blue]), C) Western green mamba (*D. viridis*) and D) Black mamba (*D. polylepis*). Data compiled from The Reptile Database (http://reptile-database.reptarium.cz) and WHO Venomous Snake Distribution Database (http://apps.who.int/bloodproducts/snakeantivenoms/database/). Photos: Wolfgang Wüster©.

Figure 2. Bayesian inference phylogenetic tree of the relationships among the five taxa of *Dendroaspis* included in this study. Node support values are Bayesian posterior clade probabilities. The relative distributions of total toxin transcripts in mamba venom gland transcriptomes are highlighted. 3FTx, three-finger toxin; KUN, Kunitz-type serine proteinase inhibitor-like; Prokin, prokineticin; PLA_2, phospholipase A_2; CRISP, cysteine-rich secretory protein; SVMP, snake venom metalloproteinase; HYA, hyaluronidase; NP, natriuretic peptide. Note the uniquely derived composition of *D. polylepis* venom compared to the green mambas among which the species is nested. **Figure 3**. Total ion current (TIC) profiles of native venom proteins of (**A**) Jameson's mamba (*D. jamesoni jamesoni*), (**B**) eastern or black-tailed Jameson's mamba (*D. j. kaimosae*) and (**C**) West African green mamba (*D. viridis*) separated by reverse-phase HPLC. Pie charts highlight the distribution of the major toxins assigned by top-down MS (3FTxs and KUN are highlighted in red and pale brown, respectively; protein sequences are listed in Supplementary Tables S9-S12). Panels **E** and **F** represent the distribution of major toxins in the revisited venom proteomes of *D. polylepis* and *D. angusticeps* [13], respectively. Protein acronyms as in Supplementary Tables S7 and S8.

Figure 4. Representative anotated top-down MS/MS spectra of the monoisotopic 7^+ topoisomers of reverse-phase HPLC peak 9 of *D. viridis* venom (m/z 6570,008) (panel **A**), and reverse-phase HPLC peak 7 of *D. viridis* venom (m/z 6569,302) (panel **B**). Mambalgin-3 [P00982] (panel **A**) and delta-dendrotoxin [C0HJB0] (panel **B**) were identified with p-values of $2.65e^{-34}$ and $5.88e^{-43}$, respectively.

Figure 5. The enzymatic PLA_2 activity of the five mamba venoms. PLA_2 activity was calculated as (U/mL)/µg venom, relative to the standard curve (see materials and methods), and then normalised across independent experimental repeats by standardising to the PLA_2 activity of the positive control (*C. atrox*). *N. melanoleuca* is included as a comparative African elapid for context. Bars represent the mean of duplicate independent experiments and the error bars represent standard deviation of the mean. Note the logarithmic scale on the y-axis.

Figure 6. The top-down MS/MS fragmentation pattern of the monoisotopic 6^+ topoisomer of *D. viridis* m/z 1127.55 ion was assigned by TopPIC either to a unknown proteoform of short α-neurotoxin S5C10 [P01419] (p-value of $9.15e^{-20}$) assuming an unexplained mass discrepancy of +242,16 Da (upper panel) or to toxin S5C10 (but with p-value of $1.46e^{-31}$) (lower panel) when the top-down data were searched against the species-specific (*D. viridis*) transcriptome. D instead of N at position 9 two additional residues (KI) at positions 50-51 fully explaind the mass difference of +242,16 Da.

Figure 7. Panel **A,** Venn diagram showing the occurrence of unique and shared intact protein masses at a given RP-HPLC retention time (MS1 feature) among mamba venoms. Panel **B**,

Principal Component Analysis. PC1 mainly differentiated *D. angusticeps* and *D.* polylepis from the Dv + (Djj, Djk) venoms by their relative abundance of toxin S5C4; PC2 further discriminated venoms by their relative abundance of DaF8 and fasciculin; and PC3 loadings separated venoms according to their relative abundance of Dendro-I/α.

Figure 8. Summary of the global immunocapturing capability of the antivenoms sampled against the venoms of the five *Dendroaspis* taxa. Columns filled with immobilised EchiTAb-Plus-ICP® and EchiTAbG antivenoms (neither of which used mamba venom as immunogens), control equine IgGs, and mock matrix were used as affinity controls. Immunocapturing capability was scored in a 0-1 scale, with 1 indicating complete (100%) retention of all venom components, and 0 negligible (0%) retention of venom components in the immunoaffinity column.

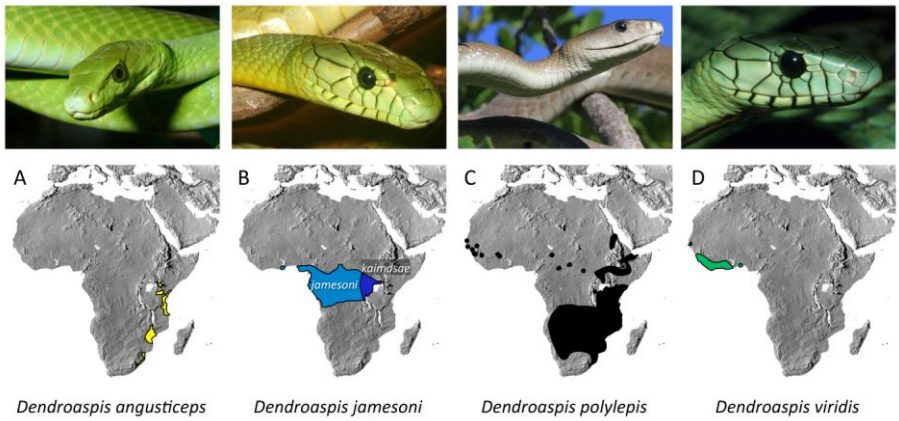

Fig. 1

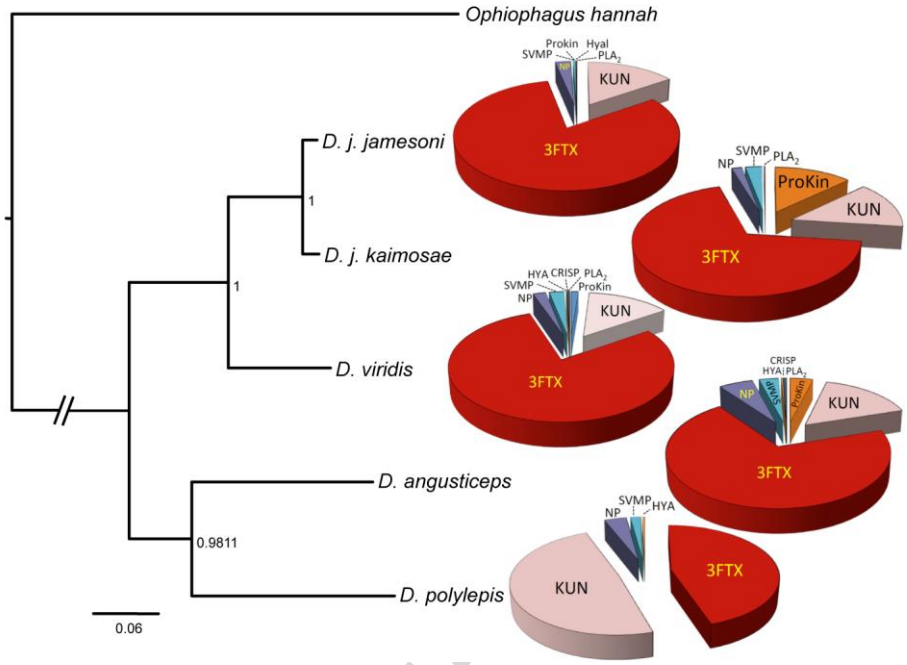

Fig. 2

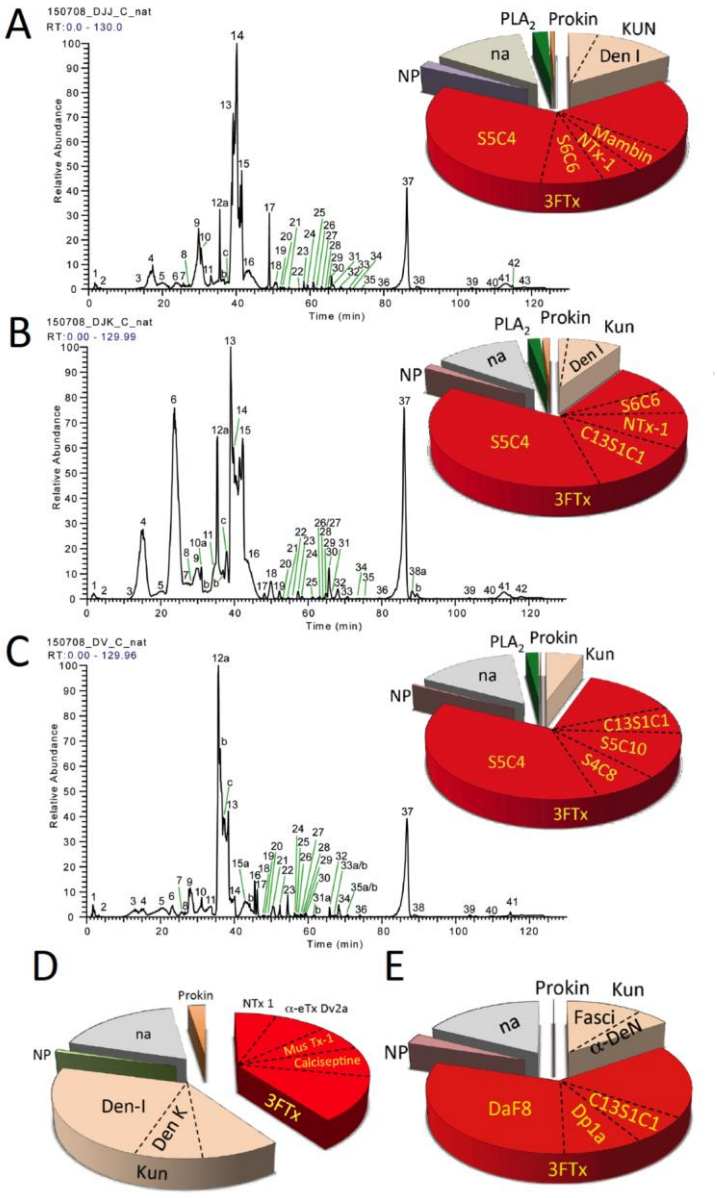

Fig. 3

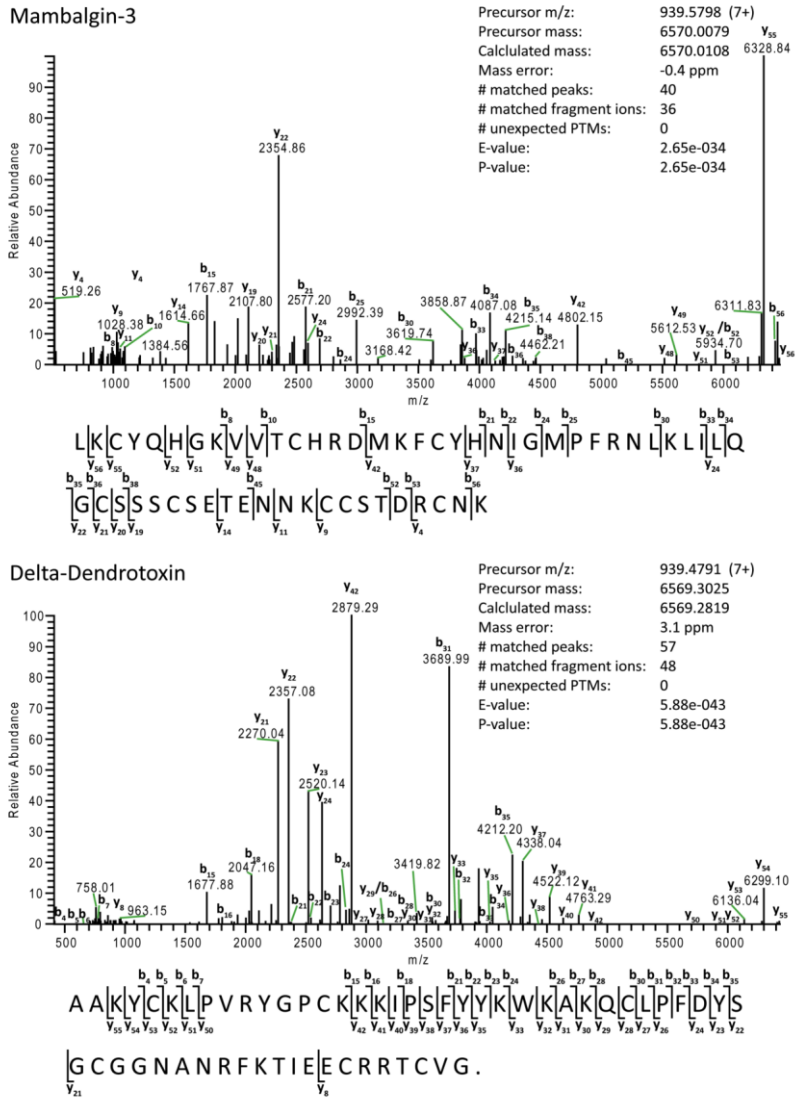

Fig. 4

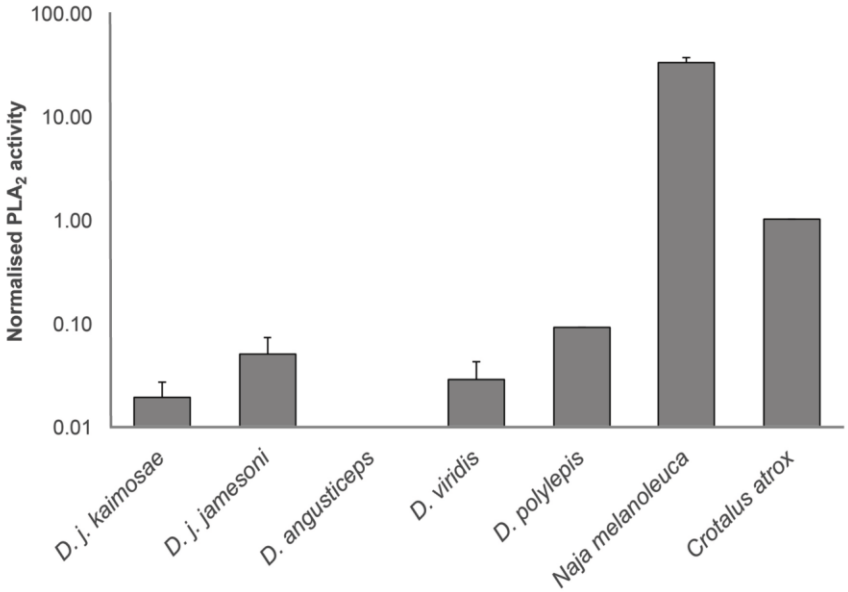

Fig. 5

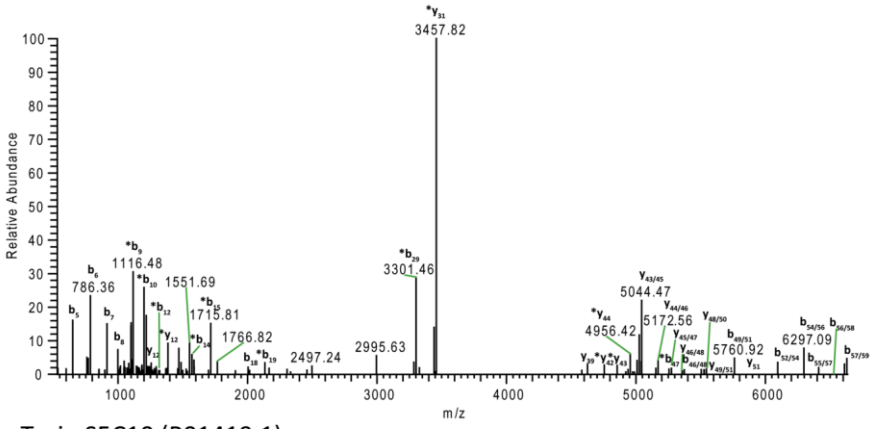

Toxin S5C10 (P01419.1)

Precursor m/z:	1127.5522 (6+)	# matched peaks:	25	E-value:	9.15e-020
Precursor mass:	6759.2696	# matched fragment ions:	21	P-value:	9.15e-020
Proteoform mass:	6759.2796	# unexpected PTMs:	1		

R I C Y N H Q S N T P A T T K S C V E +242.16 N S C Y K S I W A D H R G T I I K

R G C G C P R V K S K I K C C K S D N C N L

T0913_DV [~P01417, Toxin S5C10]

Precursor m/z:	1127.5522 (6+)	# matched peaks:	38	E-value:	1.46e-031
Precursor mass:	6759.2696	# matched fragment ions:	31	P-value:	1.46e-031
Proteoform mass:	6759.2780	# unexpected modifications:	0		

R I C Y N H Q S D T P A T T K S C V E N S C Y K S I W A D H R G T I I K

R G C G C P R V K S K I K I K C C K S D N C N L

Fig. 6

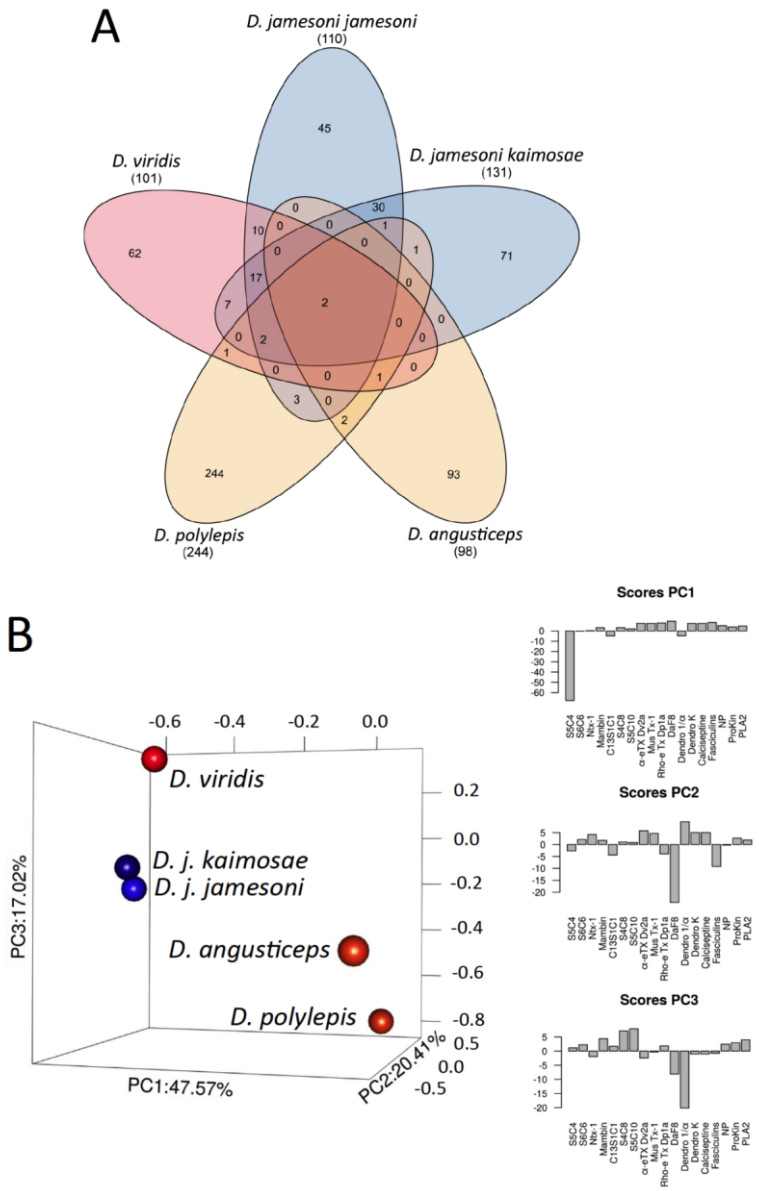

Fig. 7

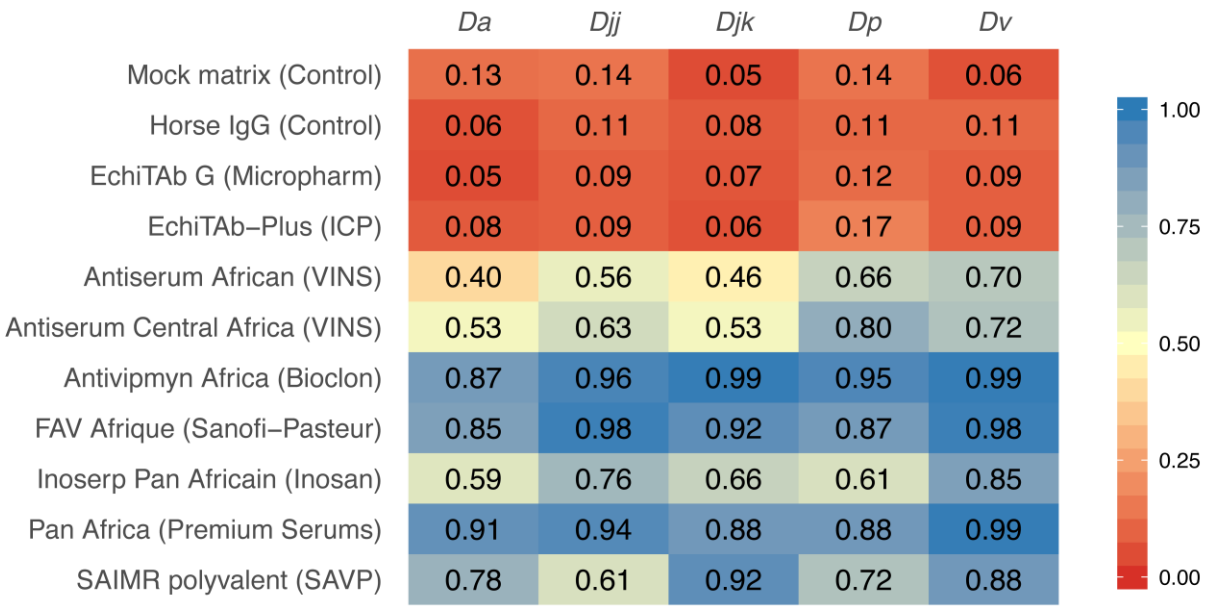

Fig. 8

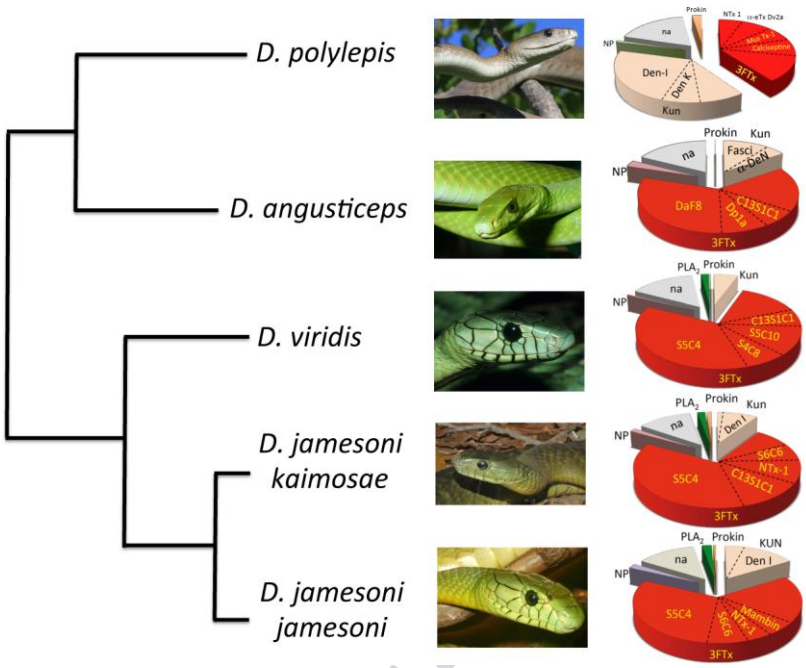

Graphical abstract

SIGNIFICANCE PARAGRAPH

The mambas (genus *Dendroaspis*) comprise five especially notorious medically important venomous snakes endemic to sub-Saharan Africa. Their highly potent venoms comprise a high diversity of pharmacologically active peptides, including extremely rapid-acting neurotoxins. Previous studies on mamba venoms have focused on the biochemical and pharmacological characterization of their most relevant toxins to rationalize the common neurological and neuromuscular symptoms of envenomings caused by these species, but there has been little work on overall venom composition or comparisons between them. Only very recently an overview of the composition of the venom of two *Dendroaspis* species, *D. angusticeps* and *D. polylepis*, has been unveiled through venomics approaches. Here we present the first genus-wide transcriptomic-proteomic analysis of mamba venom composition. The transcriptomic analyses described in this paper have contributed 29 (*D. polylepis*), 23 (*D. angusticeps*), 40 (*D. viridis*), 25 (*D. j. jamesoni*) and 21 (*D. j. kaimosae*), novel full-length toxin sequences to the non-redundant *Dendroaspis* sequence database. The mamba genus-wide venomic analysis demonstrated that major *D. polylepis* venom components are Kunitz-fold family toxins. This feature is unique in relation to the relatively conserved three-finger toxin (3FTx)-dominated venom compositions of the green mambas. Venom variation was interpreted in the context of dietary variation due to the divergent terrestrial ecology of *D. polylepis* compared to the arboreal niche occupied by all other mambas. Additionally, the degree of cross-reactivity conservation of mamba venoms was assessed by antivenomics against a panel of commercial antivenoms generated for the sub-Saharan Africa market. This study provides a genus-wide overview to infer which available antivenoms may be capable of neutralising human envenomings caused by mambas, irrespective of the species responsible. The information gathered in this study lays the foundations for rationalising the pharmacological profiles of mamba venoms

at locus resolution. This understanding will contribute to the generation of a safer and more efficacious pan-*Dendroaspis* therapeutic antivenom against any mamba envenomation.

HIGHLIGHTS

Venom gland transcriptomic and proteomic analyses across genus *Dendroaspis* are reported.

The phylogeny of *Dendroaspis* was reconstructed using gene sequences of two mitochondrial genes extracted from venom gland transcriptome data.

In contrast to other mamba venoms, which express 3FTx-predominant venoms, major *D. polylepis* venom toxins are Kunitz-type dendrotoxins.

This major difference in venom composition may reflect the divergent terrestrial ecology and mammal-dominated diet of *D. polylepis* compared to the arboreal species that prey partly or largely on birds.

Immunological profiles of the five mamba venoms against a panel of seven commercial antivenoms were assessed through antivenomics.